Evolution and Architecture of the Inner Membrane Complex in Asexual and Sexual Stages of the Malaria Parasite

Maya Kono,[1] Susann Herrmann,[2] Noeleen B. Loughran,[3,4,5] Ana Cabrera,[2] Klemens Engelberg,[1] Christine Lehmann,[1] Dipto Sinha,[1] Boris Prinz,[1] Ulrike Ruch,[1] Volker Heussler,[1,6] Tobias Spielmann,[1] John Parkinson,*[,3,4,5] and Tim W. Gilberger*[,1,2,7,8]

[1]Department of Molecular Parasitology, Bernhard Nocht Institute for Tropical Medicine, Hamburg, Germany

[2]M.G. DeGroote Institute for Infectious Disease Research, McMaster University, Hamilton, Canada

[3]Program in Molecular Structure and Function, Hospital for Sick Children, Toronto, Canada

[4]Department of Biochemistry, University of Toronto, Toronto, Canada

[5]Department of Molecular Genetics, University of Toronto, Toronto, Canada

[6]Institute of Cell Biology, University of Bern, Bern, Switzerland

[7]Department of Pathology and Molecular Medicine, McMaster University, Hamilton, Canada

[8]Department of Biochemistry and Biomedical Sciences, McMaster University, Hamilton, Canada

***Corresponding author:** E-mail: tgilber@mcmaster.ca; john.parkinson@utoronto.ca.

Associate editor: Andrew Roger

Abstract

The inner membrane complex (IMC) is a unifying morphological feature of all alveolate organisms. It consists of flattened vesicles underlying the plasma membrane and is interconnected with the cytoskeleton. Depending on the ecological niche of the organisms, the function of the IMC ranges from a fundamental role as reinforcement system to more specialized roles in motility and cytokinesis. In this article, we present a comprehensive evolutionary analysis of IMC components, which exemplifies the adaptive nature of the IMCs' protein composition. Focusing on eight structurally distinct proteins in the most prominent "genus" of the Alveolata—the malaria parasite *Plasmodium*—we demonstrate that the level of conservation is reflected in phenotypic characteristics, accentuated in differential spatial–temporal patterns of these proteins in the motile stages of the parasite's life cycle. Colocalization studies with the centromere and the spindle apparatus reveal their discriminative biogenesis. We also reveal that the IMC is an essential structural compartment for the development of the sexual stages of *Plasmodium*, as it seems to drive the morphological changes of the parasite during the long and multistaged process of sexual differentiation. We further found a *Plasmodium*-specific IMC membrane matrix protein that highlights transversal structures in gametocytes, which could represent a genus-specific structural innovation required by *Plasmodium*. We conclude that the IMC has an additional role during sexual development supporting morphogenesis of the cell, which in addition to its functions in the asexual stages highlights the multifunctional nature of the IMC in the *Plasmodium* life cycle.

Key words: Alveolata, Apicomplexa, evolution, cytoskeleton, inner membrane complex, biogenesis, gametocytogenesis.

Introduction

Plasmodium spp. are members of the Alveolata, a group of unicellular eukaryotes that incorporates the traditional phyla of Ciliates, Dinoflagellates, and Apicomplexa (Cavalier-Smith 1993). A defining feature of the Alveolata are membranous sacs underlying the plasma membrane that are termed "alveoli" in Ciliates and Dinoflagellates (Allen 1971; Lee and Kugrens 1992) or collectively "inner membrane complex" (IMC) in apicomplexan parasites (Morrissette and Sibley 2002). The flattened vesicles underlie the plasma membrane and are interconnected with the cytoskeleton.

For apicomplexans, such as *Plasmodium*, the causative agent of malaria, and other important unicellular pathogens, such as *Toxoplasma* and *Cryptosporidium*, the IMC has three major purposes: it confers stability and shape to the cell, it functions as an important scaffolding compartment during the formation of daughter cells, and it plays a major role in motility and invasion (Mann and Beckers 2001; Bergman et al. 2003; Gaskins et al. 2004; Keely and Soldati 2004; Gubbels et al. 2004; Khater et al. 2004; Baum et al. 2006; Gilk et al. 2006; de Miguel et al. 2008; Gould et al. 2008, 2011; Hu 2008; Agop-Nersesian et al. 2009; Bullen et al. 2009; Beck et al. 2010; Frénal et al. 2010; Hu et al. 2010; Lorestani et al. 2010; Tremp and Dessens 2011; Anderson-White et al. 2011). In contrast to bacteria or other parasites, apicomplexans do not hijack or rely on endocytosis-based mechanisms to enter host cells. Instead, they have developed a highly efficient machinery that connects the receptor-ligand bridge with a molecular actin–myosin motor inside the parasite. The anchoring of this so-called glideosome to the IMC membranes allows the parasite to generate the necessary force for substrate-dependent gliding and invading (Soldati et al. 2004; Baum et al. 2008).

Apart from the IMCs contribution to motility, it plays a fundamental role in maintaining cell shape and rigidity (Aikawa et al. 1981; Meszoely et al. 1987). Gametocytes of *Plasmodium* represent the nonmotile, presexual forms of the parasite that are essential for transmission from humans to the mosquito. Their development is characterized by a defined progression of morphological changes that allows a classification into five different stages (Fivelman et al. 2007). These transformations that convert a round stage I gametocyte—indistinguishable from an asexual trophozoite—into a typically crescent-shaped stage V gametocyte, are driven by alterations of the IMC and the underlying subpellicular microtubules (Sinden 1982, 1983). This highlights the principle function of the IMC as a key structural component not only of the asexual and motile stages but also for the presexual and nonmotile forms of the *Plasmodium* life cycle.

As a reflection of its multifunctionality, the IMC is composed of a diverse set of proteins. To date, 17 IMC proteins have been described in *Plasmodium falciparum*. They can be grouped according to their structural features into multitransmembrane proteins (PFE1130w, MAL13P1.130, PFD1110w, and PF14_0065), alveolins (MAL13P1.260, PFC0180c, PFC0185w, PFE1285w, PFF1035w, PF10_0039, PF11_0431, and PFL1030w), and non-alveolins (PFL1090w-GAP45, PFI0880c-GAP50, PF13_0233—MyosinA, PF14_0578, and MAL13P1.228) (Gaskins et al. 2004; Sanders et al. 2005, 2007; Baum et al. 2006; Green et al. 2006, 2008; Jones et al. 2006; Rees-Channer et al. 2006; Bosch et al. 2007; Ferguson et al. 2008; Gould et al. 2008, 2011; Tremp et al. 2008; Agop-Nersesian et al. 2009; Bullen et al. 2009; Rayavara et al. 2009; Daher et al. 2010; Frénal et al. 2010; Thomas et al. 2010; Tremp and Dessens 2011; Yeoman et al. 2011). The alveolins possess characteristic repetitive sequence motifs and were established as the first molecular nexus uniting the Alveolata (Gould et al. 2008, 2011). The emerging genomic and proteomic data from various species within the Alveolata not only exemplifies the complex and adaptive molecular composition of the pellicle and the IMC but also supports its monophylogenetic origin (Gould et al. 2011).

Toward reaching a better understanding of the complex role of the IMC in the malaria parasite, we present here an interdisciplinary analysis that combines an evolutionary investigation of the IMC with an experimental approach that focuses on eight key proteins. Our analyses suggest that the evolution of the IMC required both the recruitment and subsequent diversification of ancient eukaryotic proteins as well as the innovation of novel apicomplexan-specific proteins. We provide evidence that the IMC of the motile, asexual stages of the life cycle and the immotile, presexual stages have a connatural protein composition, despite presumably different requirements of the IMC in these respective stages. We also reveal differences in the spatial and temporal appearance of different IMC proteins that allow their classification into two protein subsets that might imply a zoning of the IMC with specific subdomains. We further show a unique structural feature of gametocytes that is defined by a *Plasmodium*-specific IMC protein, perhaps representing a cytoskeletal innovation required for sexual development in this genus.

Materials and Methods

Data Collection

Inparanoid (Remm et al. 2001; O'Brien et al. 2005; Berglund et al. 2008) searches for each of the 17 IMC proteins of interest were performed against a set of 120 complete eukaryotic genomes to identify an initial set of orthologous sequences (seed data). Individual multiple sequence alignments (MSAs) were generated using MUSCLE v3.6 (Edgar 2004). The 17 resultant MSAs were manually edited to remove any ambiguity using Se-Al v2.0a11 (Rambaut et al. 1996). Hidden Markov Model (HMM) profiles were constructed from each of the MSAs using HMMER3 (Eddy 2009). Using these profile HMMs and the HMM search algorithm implemented in HMMER3, remote homologs (E value 1×10^{-5}) for each of the 17 protein families were identified across four independent databases: 1) PhyloPro (Xiong et al. 2011): the original set of 120 complete eukaryotic genome, 2) Ensembl (Flicek et al. 2011): database version 61, 3) PartiGeneDB (Peregrin-Alvarez et al. 2005): a group of ~700 peptide data sets generated from collections of expressed sequence tags (ESTs), and 4) the nonredundant NCBI protein sequence database. Comprehensive data sets for each protein family were generated using these newly identified homologs and the initial seed data. Redundancy within these data sets was removed using the CD-HIT program (Huang et al. 2010). In these analyses, we found PF13_0233, a myosin class protein, to be ubiquitous across the Eukarya with ~300 orthologs detected through InParanoid searches and a further 500 identified through HMM searches. Due to its high level of conservation, this protein family was excluded from further downstream analyses.

Homology Network and Phylogenetic Analysis

The initial seed data together with the remote homologs identified through HMM searches of the PhyloPro (Xiong et al. 2011) database were used in the construction of a homology network of IMC-associated proteins. Any redundancy within this combined data set was removed as above prior to performing all-versus-all searches using the Needleman–Wunsch algorithm. Global alignment scores were used to construct a homology network, which was visualized using Cytoscape (Shannon et al. 2003). An MSA for the six-transmembrane proteins was generated and refined as above prior to phylogenetic reconstructions. For the Alveolin metanetwork, three alignments were generated using MUSCLE v3.6 (Edgar 2004): 1) the entire MSA for the data, 2) an MSA of only the alveolin repeat regions, and 3) an MSA of only the flanking regions. TrimAl (Capella-Gutierrez et al. 2009) was used to automatically remove columns of the alignments with a gap threshold of 0.95 and manually edited using Se-Al v2.0a11 (Rambaut

et al. 1996). The optimum model of amino acid substitution for each data set was determined using ModelGenerator v0.85 (Keane et al. 2006). The likelihood mapping approach implemented in TREE-PUZZLE v5.2 (Schmidt et al. 2002) was used to assess the level of phylogenetic signal/conflict in each data. An initial maximum likelihood (ML) phylogeny for the Alveolin metanetwork was reconstructed based on 1) and 2) above (no phylogenetic signal was present in 3)) using PhyML (Guindon and Gascuel 2003) with 1,000 bootstrap replicates which allowed the identification of three subgroups which were than subjected to more robust phylogenetic analyses. ML (with 1,000 bootstrap replicates) and Bayesian phylogenies (MrBayes 3.1.2, Ronquist and Huelsenbeck 2003), using four Markov chains for 3 million generations with a burnin of 80,000, were reconstructed for the six-transmembrane metanetwork and each alveoli subgroup (note the alveolin metanetwork alignment approach was taken for each alveolin subgroup—with no phylogenetic signal detected in the flanking regions alone) using the predetermined substitution model. A comparison of both the ML and Bayesian trees was performed using the Shimodaira–Hasegawa test (Ota et al. 2000) implemented in TREE-PUZZLE v5.2 (Schmidt et al. 2002) to determine which tree was significantly the best-fit tree for the corresponding MSA.

Cell Culture and Transfection of *P. falciparum*

Plasmodium falciparum (3D7) was cultured in human O+ erythrocytes according to standard procedures using complete Roswell Park Memorial Institute (RPMI) medium (Trager and Jensen 1976). Gametocytes were produced using a modified version of the established protocol (Fivelman et al. 2007). 3D7 wild-type and transgenic cell lines were synchronized with 5% sorbitol and cultivated at a parasitemia of 1% under standard conditions. Synchronized gametocytogenesis was evoked by starvation of the fast-growing culture by renewing only 2/3 of the culture media. This procedure was repeated for the next 10–12 days, and the sexual stages were harvested at different time points using MACS separation columns (Miltenyi Biotec, Germany).

For transfection, ring-stage parasites (10%) were electroporated with 100 μg of plasmid DNA resuspended in cytomix as previously described. Transfectants were selected using 10 nM WR99210 (Fidock and Wellems 1997). Double transfectant parasites expressing MAL13P1.130-GFP and GAP45-mCherry or PF10_0039-mCherry were generated by transfecting 100 μg of pB-GAP45-mCherry or pB-PF10_0039-mCherry plasmid DNA into the transgenic MAL13P1.130-GFP cell line. Double transfectant parasites expressing PF14_0578-mCherry and PfCentrin3 were generated by transfecting 100 μg of pB-PF14_0578-mCherry into the transgenic *Pf*Centrin3-GFP cell line. Selection was carried out using 10 nM WR99210 and 30 nM blasticidin.

Transfection of *Plasmodium berghei*

Plasmodium berghei (ANKA) parasites were transfected using a *Apa*I- and *Sac*II-linearized transfection plasmid as previously described (Janse et al. 2006). NMRI strain mice, between 6 and 10 weeks of age, were supplied by Charles River Laboratories or bred in house at the Bernhard Nocht Institute for Tropical Medicine. Experiments were conducted in accordance with European regulations and approved by local authorities.

In Vitro Infection of HepG2 Cells

Human hepatoma cells (HepG2) were obtained from the European Cell Cultures Collection. Cells were cultivated at 37 °C and 5% CO_2 in Eagle's minimal essential medium (EMEM) media (PAA) containing 10% fetal calf serum, 2 mM L-glutamine, 100 U/ml penicillin, and 100 mg/ml streptomycin (all PAA Laboratories GmbH). For infection, approximately 50,000 cells were seeded per cover slip in a 24-well plate. *Plasmodium berghei* (ANKA) sporozoites were prepared from salivary glands of infected *Anopheles stephensi* mosquitoes and incubated with HepG2 cells in EMEM (PAA) containing 3% bovine serum albumin (BSA) (Sigma), 2 mM L-glutamine, 100 U/ml penicillin, and 100 mg/ml streptomycin (all PAA Laboratories GmbH) at 37 °C and 5% CO_2. After 2 h, cells were washed and fresh culture medium was added.

Nucleic Acid and Constructs

PFE1130w, MAL13P1.130, PFD1110w, PF10_0039, PFE1285w, MAL13P1.228, and PF14_0578 were previously cloned as green fluorescent protein (GFP) fusions (Hu et al. 2010). Full-length PF10_0271 (*Pf*Centrin3) was cloned into pARL-GFP (Treeck et al. 2006). The pB-GAP45-mCherry as well as the pB-PF10_0039-mCherry and pB-PF14_0578-mCherry plasmids were generated by modifying the expression plasmid pBcamR (Flueck et al. 2010): The Rep20 repeat sequence and the *cam*-promotor were replaced by the late stage specific *ama-1* promotor using PstI/BamHI restriction sites. The 3xHA tag of the original vector was replaced by mCherry using NotI/SalI cut sites. Genes were cloned into BamHI/SalI sites of the pB-mCherry vector. All oligonucleotides are listed as supplementary data table 1 (Supplementary Material online). The GFP replacement construct for tagging the endogenous MA13P1.130 was designed using the pH vector. This vector was derived from the pHcam1005-3xHA vector (Voss et al. 2006), where the 3xHA tag was exchanged for GFP. The full-length *MAL13P1.130* gene was cloned into the PstI/SalI sites, replacing *rep20*, *cam*-Promotor, and as well as *PFL1005c*. The transfected parasites were subject to four cycles of growth in the presence or absence (6 weeks) of 10 nM WR99210. The orthologs of MAL13P1.130 and PFE1285w in *P. berghei* were identified in PlasmoDB. They were amplified using cDNA of *P. berghei* ANKA wild-type mixed blood stage parasites and the oligonucleotides summarized in supplementary data table 1 (Supplementary Material online). The open reading frames with additional 1-kb upstream region were cloned into the pl0017 vector (obtained through the MR4 (MRA-786)) using EcoRV/BamHI cut sites to allow the expression of GFP-fusion proteins under their endogenous promoters.

For the production of Glutathion-S-Transferase (GST)-fusion protein, 334 bp of the C-terminus of PFD1110w was polymerase chain reaction (PCR) amplified and cloned into pGEX-4T-1 using the BamHI/NotI restriction sites (supplementary data table 1, Supplementary Material online). All PCR amplifications were performed using Phusion DNA polymerase (New England Biolabs).

Recombinant Expression and Antiserum

Expression and purification of PFD1110w-GST *Escherichia coli* (BL21) was done according to manufacture recommendation (GE Healthcare) using glutathione sepharose 4B (Amersham Biosciences) and used for immunization of mice (Eurogentec).

Imaging and Immunofluorescence Assays

All fluorescence images were observed and captured using either a Zeiss Axioskop 2plus microscope with a Hamamatsu Digital camera (Model C4742-95) or the Olympus FV1000 confocal microscope. For confocal images and 3D reconstitution, 20–32 z-stacks (0.38 μm step size) were collected using 488 or 594 nm lasers. All confocal images were analyzed and processed in Imaris 6.2.0. Cropping of movies and addition of time stamps were carried out in ImageJ (http://rsb.info.nih.gov/ij/). Gauss filters were used with the filter width suggested by Imaris. Single images were processed in Adobe Photoshop CS4. For long-term observations, parasites were arrested using culture grade 0.5 mg/ml concanavalin A (Sigma) on glass bottom 35 mm dishes (Ibidi) and viewed at 37 °C using an Olympus FV1000 confocal microscope (488 nm) equipped with an Olympus Cellcubator as previously described (Grüring et al. 2011). Image collection parameters were 4 μs dwell time, 512 × 512 dpi, 16–32 z-stacks (0.2–0.4 μm step size), and zoom level of 1–7 and laser levels of 1–5% for 488 nm.

Immunofluorescence assays were performed using fixed *P. falciparum* parasites as previously described (Tonkin et al. 2004). All primary antibody dilutions were prepared in 3% BSA. Mouse anti-PFD1110w was diluted 1:250, anti-alphatubulin 1:2000 (Molecular Probes), and anti-Pfs16 1:1500. Secondary antibodies (Alexa-Fluor 594 goat anti-rabbit IgG antibodies and Alexa-Fluor 594 goat anti-mouse IgG antibodies, Molecular Probes) were diluted 1:2000 with a DAPI (Roche) concentration of 1 μg/ml also in 3% BSA.

Plasmodium berghei blood stages were imaged using peripheral blood samples taken 7–14 days post-infection. *Plasmodium berghei* sporozoites infected HepG2 cells were fixed with 4% formaldehyde in phosphate-buffered saline (20 min, room temperature), permeabilized with ice-cold methanol (10 min), and after 30 min of blocking with 5% Fetal Calf Serum (FCS) incubated with the appropriate primary antibodies. Mouse anti-GFP was diluted 1:1000 (Molecular Probes) and anti-Circumsporozoite protein (CSP) 1:1000 (Eurogentec) in 5% FCS. Subsequently, the samples were incubated with secondary antibodies (Alexa-Fluor 594 goat anti-rabbit IgG antibodies and Alexa-Fluor 594 goat anti-mouse IgG antibodies, 1:2000, Molecular Probes). DNA was visualized by staining with 1 μg/ml DAPI (Sigma).

Ookinetes were enriched using whole blood samples from mice with high parasitemia and amount of gametocytes. The sample was incubated in ookinete media (RPMI 1640, 1 g/l Na_2CO_3, 5 U/ml Penicillin, 5 μg/ml Streptomycin, 100 μM xanthurenic acid, pH 7.4) over night at 19 °C and 96% humidity. Differentiated ookinetes were visualized the next day.

Results

In addition to helping define apicomplexan cell morphology, IMC proteins play a fundamental role in host cell invasion as well as cytokinesis. Despite their importance, little is currently known about how the various components of the IMC are organized and operate as a highly specialized system unique to Apicomplexa. In the first section of this study, we focus on an evolutionary analysis of the IMC in an attempt to explore its origins, as well as identify lineage-specific innovations (e.g., associated with distinct host cell invasion strategies). These evolutionary analyses serve to complement our systematic investigation that focuses on eight key proteins and their dynamics during several key stages of the *Plasmodium* life cycle.

A Group of Structurally Distinct and Phylogenetically Diverse Proteins Define the IMC

To examine the evolutionary trajectories of all known IMC proteins in the malaria parasite, we first performed a systematic search for putative homologs (see Materials and Methods). These searches revealed that the 16 structurally diverse IMC proteins (fig. 1A—PF13_0233 was excluded from these analyses as it is extremely well conserved) display a mosaic pattern of evolutionary trajectories, from those that are highly conserved across eukarya (e.g., PFE1130w) to those that appear specific to the Apicomplexa (e.g., PFF1035w) and even one gene which appears limited to the genus *Plasmodium* (MAL13P1.228, fig. 1B). In these analyses, we identified an additional six *P. falciparum* homologs that were not previously associated with the IMC and may play additional roles in this structure (PF08_0033, PF14_0168, PF08_0013, PF07_0031, PF14_0614, and PF10_0107). Consistent with a previous study, the three six-transmembrane proteins are restricted to the Apicomplexa (Bullen et al. 2009). However, the alveolins are associated with a more diverse pattern of conservation. PFE1285w appears well conserved across eukarya, whereas PFF1035w and MAL13P1.260, like the six-transmembrane proteins, are restricted to the Apicomplexa. Intriguingly, three alveolins (PFC0180c, PFL1030w, and PF10_0039) are predicted to have orthologs in several insect species but not in other taxa outside Apicomplexa suggesting that these genes may have been acquired or donated through lateral gene transfer.

With the systematic assemblage of IMC proteins and their homologs, we were next concerned with identifying putative evolutionary relationships between the various components as well as identifying lineage-specific differences that may reflect taxon-specific innovations (e.g., altered host cell invasion strategies). As a first step, we performed

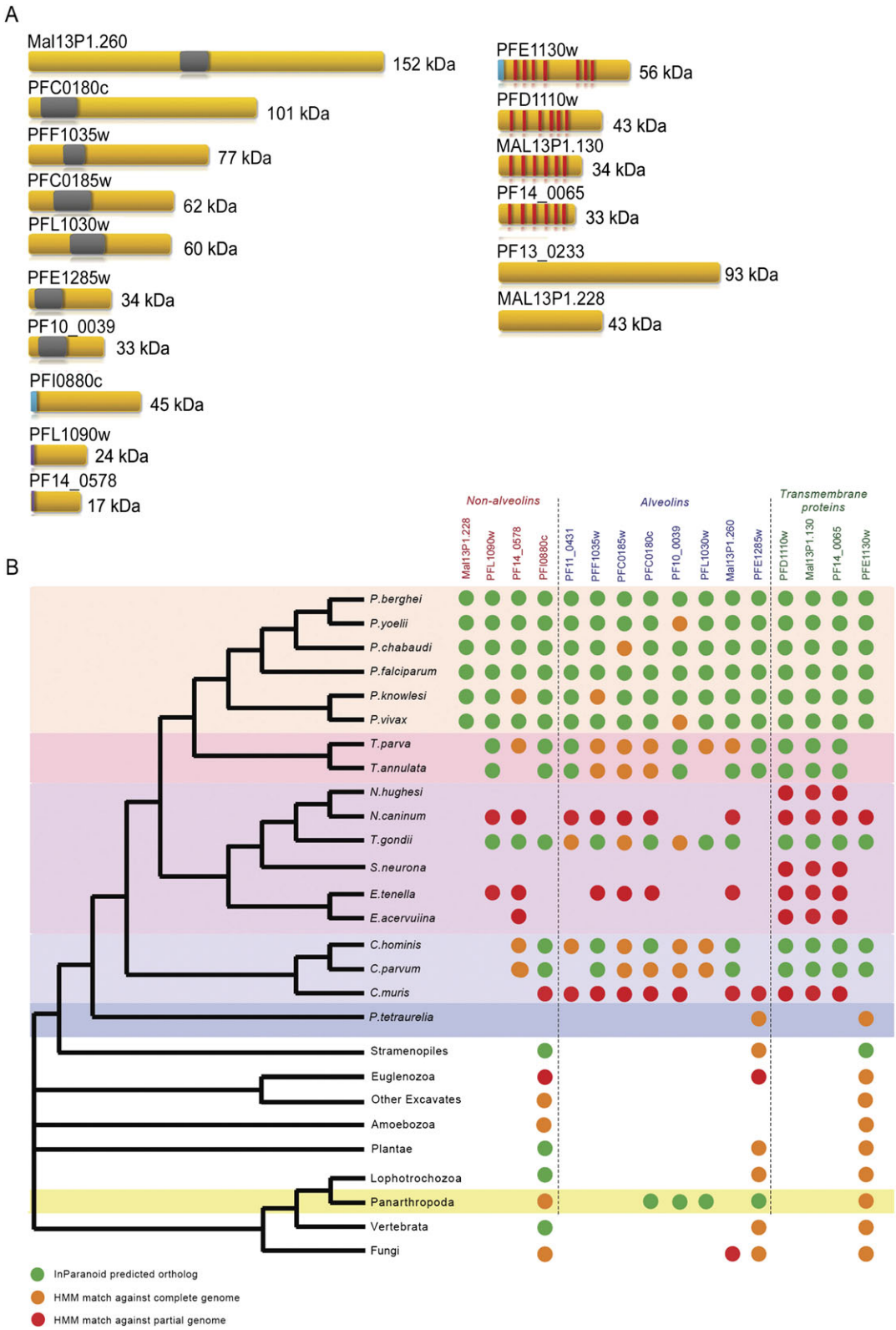

FIG. 1. Structural and phylogenetic characterization of IMC proteins. (*A*) Schematic representation and putative functional domains of the 17 known IMC proteins forming three distinct groups. Signal peptides: blue; transmembrane domains: red; alveoline domains: gray; lipid modification motifs: purple (*B*). Taxonomic distribution of IMC proteins. From a series of comprehensive and systematic sequence searches, we identified putative homologs of the IMC genes targeted in this study. Green circles indicate orthologs from a single species identified through genomic comparisons using the software tool InParanoid. Orange circles indicate the lack of an InParanoid-predicted ortholog, but the presence of a homolog based on an HMM search against the genome. Red circles indicate the lack of an InParanoid-predicted ortholog or homolog based on an HMM search against the genome, but the presence of a putative homolog based on comparisons to EST data sets. Note: PF13_0233 was excluded due to its ubiquitous nature across the eukaryotes.

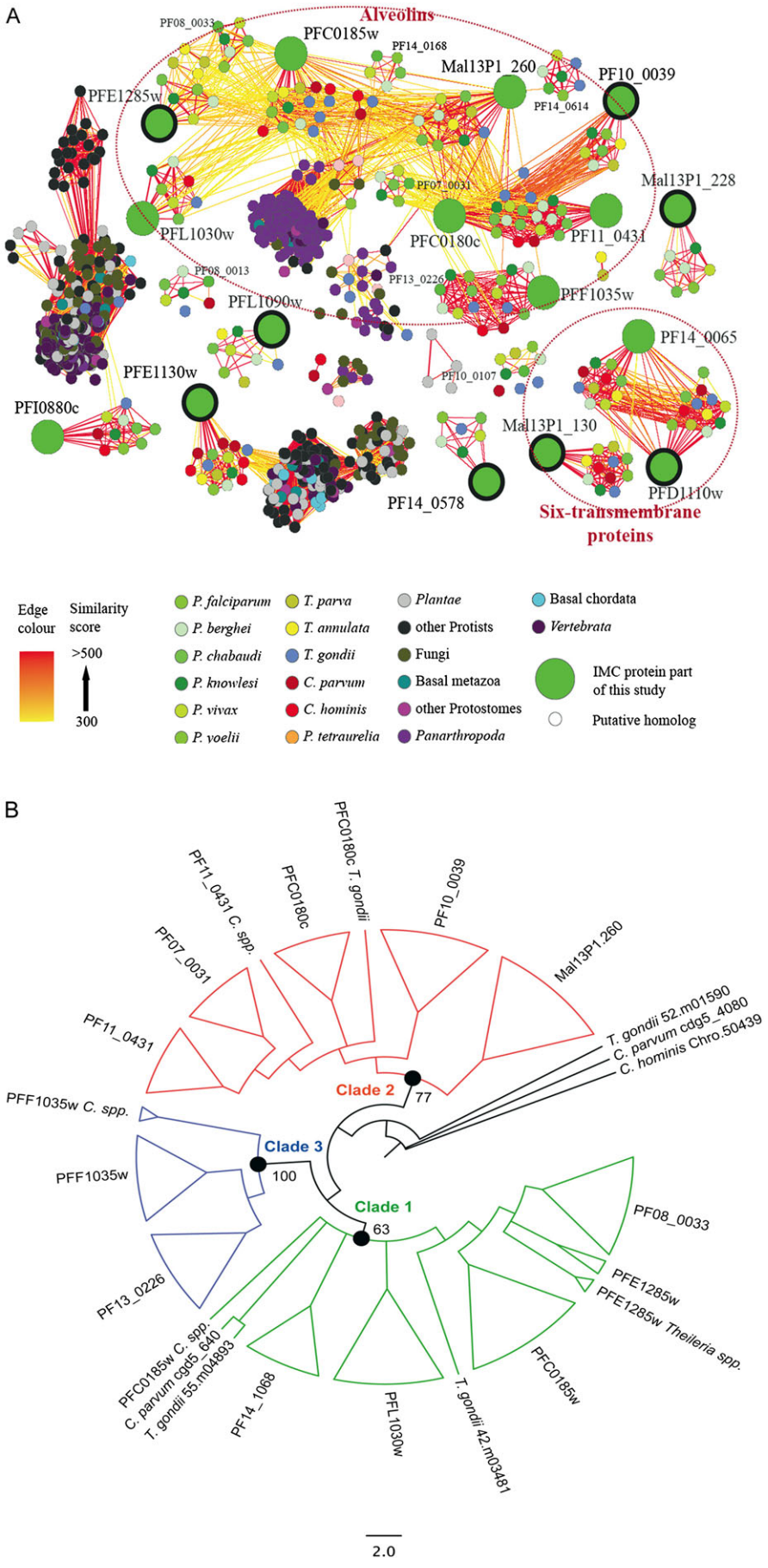

a series of pairwise global sequence alignments to construct an IMC-specific homology network (fig. 2*A*). The construction of such networks allows the identification of consistent patterns of gene conservation as well as highlighting lineage-specific gains and losses (On et al. 2010). In addition, although homology networks do not substitute for more robust phylogenetic analyses, they have been used as a robust framework to define gene families which serve to guide which taxa should be considered for inclusion in such analyses (Li et al. 2003; Chen et al. 2006). In general, each IMC protein is associated with a distinct cluster composed of closely related sets of homologs from other Apicomplexa. The lack of inclusion of species from outside this phylum reflects the relative divergence of these proteins. Furthermore, within each cluster, each species tend to be represented by a single gene copy, although examples of lineage-specific gains and losses are evident. For example, we note the inclusion of two *Toxoplasma gondii* homologs in the MAl13P1.130 cluster, which were confirmed as paralogs in subsequent phylogenetic analyses (see below).

The global homology network also reveals that although the non-alveolin and seven-transmembrane protein (PFE1130w) clusters are distinct from the rest of the network, the three six-transmembrane proteins and alveolins comprise two unrelated metanetworks. Within the six-transmembrane metanetwork, the Mal13P1.130 group of sequences appears more divergent than those from the other two clusters. This was further supported by more robust phylogenetic analysis, which also established the occurrence of two *T. gondii* orthologs in each of the PFD1110w and MAl13P1.130 families (supplementary fig. 1*A*, Supplementary Material online). It should be noted, however, that due to the absence of additional homologs from outside the Apicomplexa, it was not possible to root the tree and thus reconcile the evolutionary history of this metanetwork.

To gain insights into the evolutionary relationships among the alveolins, we performed an initial ML analysis on the alveolin metanetwork (fig. 2*B*). Two analyses were performed based on 1) the MSA for the entire proteins and 2) an MSA of only the core alveolin repeat regions (supplementary text 1, Supplementary Material online). The overall topology of 1) and 2) was congruent highlighting the influence of the alveolin repeat region on phylogenetic signal. Due to the repetitive nature of these sequences, care must be taken in inferring evolutionary relationships on the basis of this global analysis. Nevertheless, based on bootstrap support, this topology allowed for the identification of three alveolin clades, which were subjected to independent phylogenetic analysis to further improve resolution of evolutionary relationships.

In each of these analyses, two reconstructions were performed based on 1) the entire protein sequence and 2) the core alveolin regions. Both types of analyses resulted in only superficial species rearrangements within protein families (supplementary fig. 1*B–D*, Supplementary Material online). The first clade (supplementary fig. 1*B*, Supplementary Material online) includes the previously characterized alveolins: PFC0185w, PFE1285w, PFL1030w, as well as PF14_0168 (a conserved hypothetical protein) and PF08_0033 (annotated as "membrane skeletal IMC1-related"). PF08_0033 and PFE1285w represent paralogs as do PFL1030w and PFC0185w. With the absence of orthologs from other species, the PF08_0033 and PFE1285w families likely arose in the Aconoidasida lineage prior to the split of the Haemospordia from the Piroplasmida. Intriguingly, PFL1030w appears to represent an ancestral apicomplexan duplication, which has been lost in the Piroplasmida suggesting that this gene is dispensable for the invasion strategies within this lineage. It is further interesting to note that PF14_0168 was the only IMC protein family that demonstrated a species-specific gain/loss within the *Plasmodium* lineage (lost in *P. knowlesi*). The second clade includes PFC0180c, PF10_0039, PF07_0031, PF11_0431, and MAL13P1.260; the first four families appearing more closely related (supplementary fig. 1*C*, Supplementary Material online). The position of a putative *Cryptosporidium* spp. ortholog in the PF11_0431/PF07_0031 lineage, together with the absence of such orthologs in PF10_0039, PFC0180c, and MAl13P1.260 clade, might indicate multiple lineage-specific loss events. On the other hand, without a defined outgroup, the *Cryptosporidium* representative may simply represent an ortholog to all families within this clade and should therefore occupy a more basal position within the tree. Therefore, it may be speculated that PF11_0431, PF07_0031, and PFC0180c represent Haemosporidia-specific expansions. The third clade (supplementary fig. 1*D*, Supplementary Material online) includes PFF1035w together with PF13_0226, a conserved apicomplexan protein of unknown function, which resolve into two distinct clades. The position of orthologs from the *Cryptosporidium* lineage suggests that these two alveolin clades represent a duplication event that occurred sometime between the split of the *Cryptosporidium* and *Coccidian*

Fig. 2. Sequence comparisons of IMC proteins. (*A*) Homology network of IMC-associated proteins. The network shows sequence similarity relationships between 984 proteins identified through InParanoid comparisons and HMM searches against genome data sets. Nodes indicate proteins and links indicate shared sequence similarity based on Needleman–Wunsch global alignment scores (NB only scores greater than 300 are shown, and hence, some proteins may appear disconnected from the network if the scores are below this threshold). *P. falciparum* proteins targeted in this study are highlighted in green—those which have been experimentally investigated have a thick border. Colors of nodes indicate taxonomic origin of protein. The Cytoscape file used to visualize the network is made publically available for download from our project website: http://www.compsysbio.org/projects/apicomplexa/. (*B*) ML tree of alveolins based on the metanetwork. Numbers indicate % bootstrap support (from 1,000 samplings). Based on this tree, three clades (highlighted by black circles) were defined for further phylogenetic investigation (supplementary fig. 1*B–D*, Supplementary Material online).

lineages. In addition, representatives from the Piroplasmida lineage are also lacking. Although the homology network (fig. 2A) identified two potential homologs in *Theileria parva* and *T. annulata* (XP_765473.1 and XP_951812.1, respectively), only the *T. annulata* protein was found to share weak sequence similarity with this clade (a single significant sequence match to the *P. yoelii* ortholog of PFF1035w). Thus, even if related, these *Theileria* proteins likely perform distinct roles to those from the other apicomplexans.

From these analyses, it is clear that the innovation of the IMC by the Apicomplexa has required both the recruitment and subsequent diversification of ancient eukaryotic proteins, together with the emergence of new apicomplexan-specific proteins. Although examples of lineage-specific duplications and losses are apparent, the majority of the IMC proteins display consistent 1:1 orthologous relationships, particularly within the *Plasmodium* lineage, suggestive of core-conserved functionality. In the following analyses, we next present findings from a series of in depth cell localization studies that attempt to gain further insights into the organization and function of eight selected members of the IMC with diverse phylogenetic distributions.

Differential Spatial Distribution of IMC-Resident Proteins during Schizogony

To deepen our understanding of the dynamic and putative subcompartmentalization of the IMC during blood-stage schizogony of the malaria parasite, we used the transmembrane proteins PFE1130w, MAL13P1.130 and PFD01110w, the alveolins PF10_0039 and PFE1285w, the non-alveolins MAL13P1.228 and PF14_0578, and the well-characterized glideosome protein PFL1090w (GAP45) for localization studies and some selected ones for time-lapse microscopy. As noted above, these proteins have a diverse phylogenetic background: PFE1285w and PFE1130w appear to have ancient origins, MAl13P1.228 appears to be a recent *Plasmodium* specific innovation, whereas the rest are associated with the emergence of the *Apicomplexa*. Furthermore, the proteins have miscellaneous structural features and membrane attachment mechanisms (fig. 1) but are cotranslationally expressed and predicted to be involved in invasion by PlasmoINT (Hu et al. 2010). Therefore, they were expressed under the control of the *ama1*-promotor that mimics their endogenous expression profile. This approach was validated by using 1) specific antibodies (supplementary data S2, Supplementary Material online), 2) exchanging the *ama1*-promotor with the endogenous promotor (supplementary fig. 3*A* and *B*, Supplementary Material online), and 3) by replacing the endogenous 3′end with GFP (supplementary fig. 3*C*–*G*, Supplementary Material online). All three complementary approaches show an undistinguishable dynamic during schizogony and sexual differentiation for the individual IMC proteins as described below.

The transmembrane proteins (PFE1130w, MAL13P1.130, and PFD1110w) and the non-alveolin protein (PF14_0578) show a previously described dynamic (Bullen et al. 2009; Rayavara et al. 2009; Hu et al. 2010; Yeoman et al. 2011) during schizogony. These proteins mark cramp-like structures (Hu et al. 2010) that show a 2:1 numerical correlation with the nuclei at the onset of schizogony representing the first sites of the two developing merozoites (fig. 3*A*, T1). Tangential sectioning using confocal microscopy and 3D reconstructions reveals the orientation of these structures toward the periphery of the schizont. These structures develop to ring-like formations with an average diameter of 630 ± 100 nm (fig. 3*A*, T2; fig. 3*B*; and supplementary movie S1, Supplementary Material online), which toward the end of schizogony appear to quickly expand toward the posterior end of the nascent merozoites reflecting the growth of the IMC beyond the nuclei (fig. 3*A*, T3). This dynamic distribution pattern is identical with that of the established IMC marker protein GAP45 (fig. 3*C*) as shown in the GAP45-mCherry expressing parasite line as well as in a double transgenic parasite line expressing GAP45-mCherry and MAL13P1.130-GFP (fig. 3*D*). Given the similar localization patterns of these proteins and to differentiate them from other IMC proteins, we subsequently refer to them as "group A" proteins.

To further analyze the nucleation of the nascent IMC, the centrosome marker protein *Pf*Centrin3 (PF10_0271, Mahajan et al. 2008) was expressed as a GFP-fusion protein and coexpressed with the group A protein PF14_0578 as an mCherry chimera (fig. 3*E*, supplementary movie S3, Supplementary Material online). From the onset of the IMC biogenesis, an association of Centrin3 with the nascent IMC can be visualized placing it in the center of the developing IMC structure (fig. 3*E*, T1-2 and supplementary movie S4, Supplementary Material online).

In contrast, the two alveolins PF10_0039 and PFE1285w and the non-alveolin MAL13P1.228 can be distinguished by the initial formation of thin ring-like structures in midstage schizonts (fig. 4*A*, T1 and supplementary movie S2, Supplementary Material online). We, therefore, subsequently refer to these as "group B" proteins. With 900 ± 100 nm diameters, these rings have a considerably larger dimension (fig. 4*B*, T1) than the group A counterparts (fig. 3*B*, supplementary movie S2, Supplementary Material online). Furthermore, group B proteins do not display the cramp-like structures formed by group A proteins, prior to the formation of the ring structure. These apparent different dynamics were further analyzed by colocalization studies using two different pairs of group A or B proteins. First, immunofluorescence-based microscopy was applied using antibodies raised against the group A protein, PFD1110w. Antibody specificity was confirmed in wild-type parasites as well as in PFD1110w-GFP overexpressing transgenic parasites (supplementary fig. S2, Supplementary Material online). Importantly, the expression pattern of the endogenous protein and its ectopically expressed GFP-fusion version were identical (supplementary fig. S3*A* and *B*, Supplementary Material online). Subsequent colocalization studies with PFE1285w-GFP (group B) showed an intriguing spatial relation (fig. 4*C*, T1-3). A strict polarity along the longitudinal axis of the nascent merozoite is

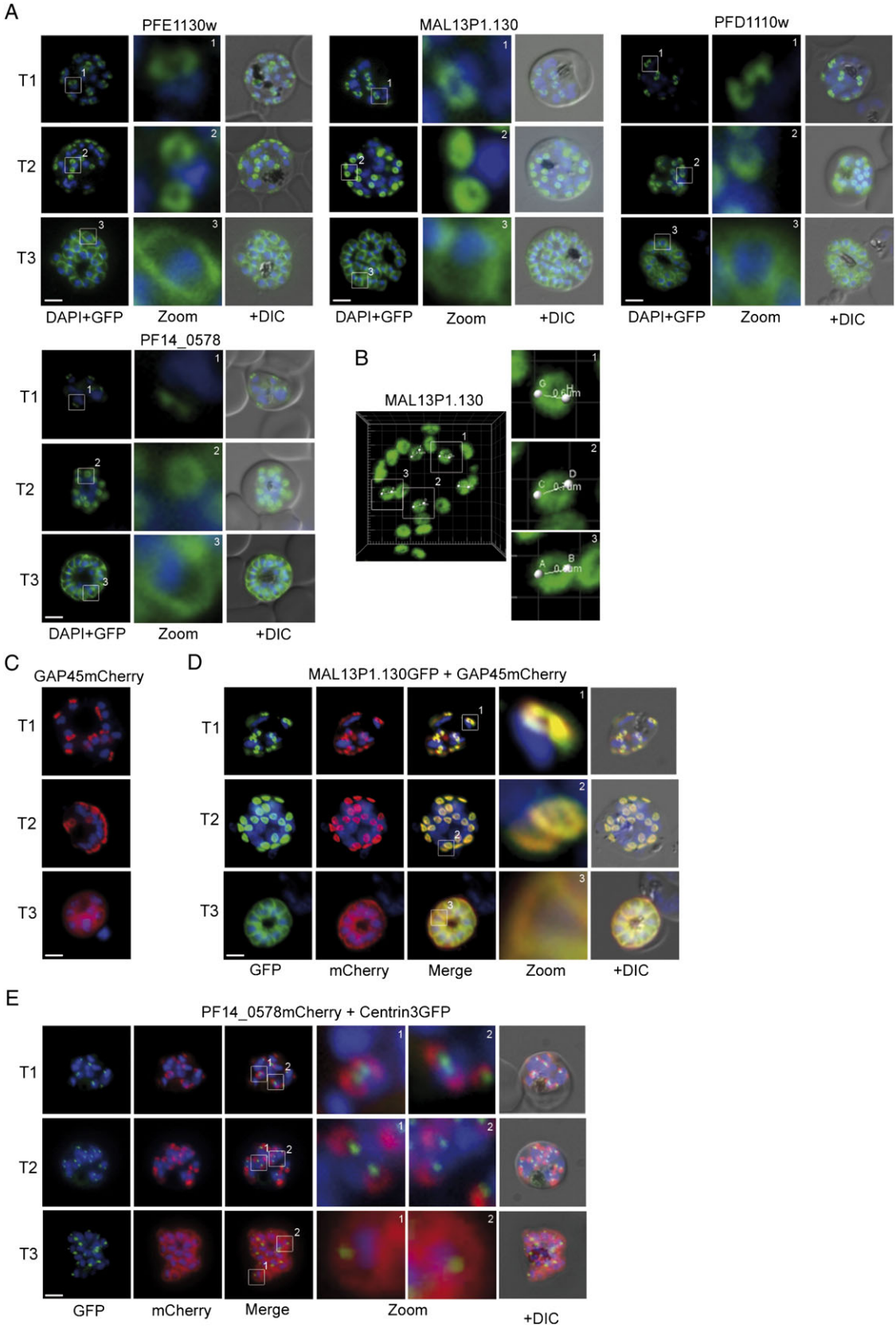

Fig. 3. Group A–associated proteins colocalize with GAP45 during schizogony. (*A*) Using GFP as a fluorescence tag, the TMD proteins PFE1130w, MAl13P1.130, PFD1110w, as well as PF14_0578 reveal three distinct structures during ongoing schizogony. Commencing as cramp-like structures (T1), they transform to small ring-shaped formations (T2) that toward the end of schizogony expand and are then equally distributed underneath the plasma membrane (T3). Enlargement of these distinct structures are marked (white square) and shown in second row (Zoom) for each cell line. (*B*) The ring structures highlighted by the TMD proteins and PF14_0578 have a maximum average diameter of

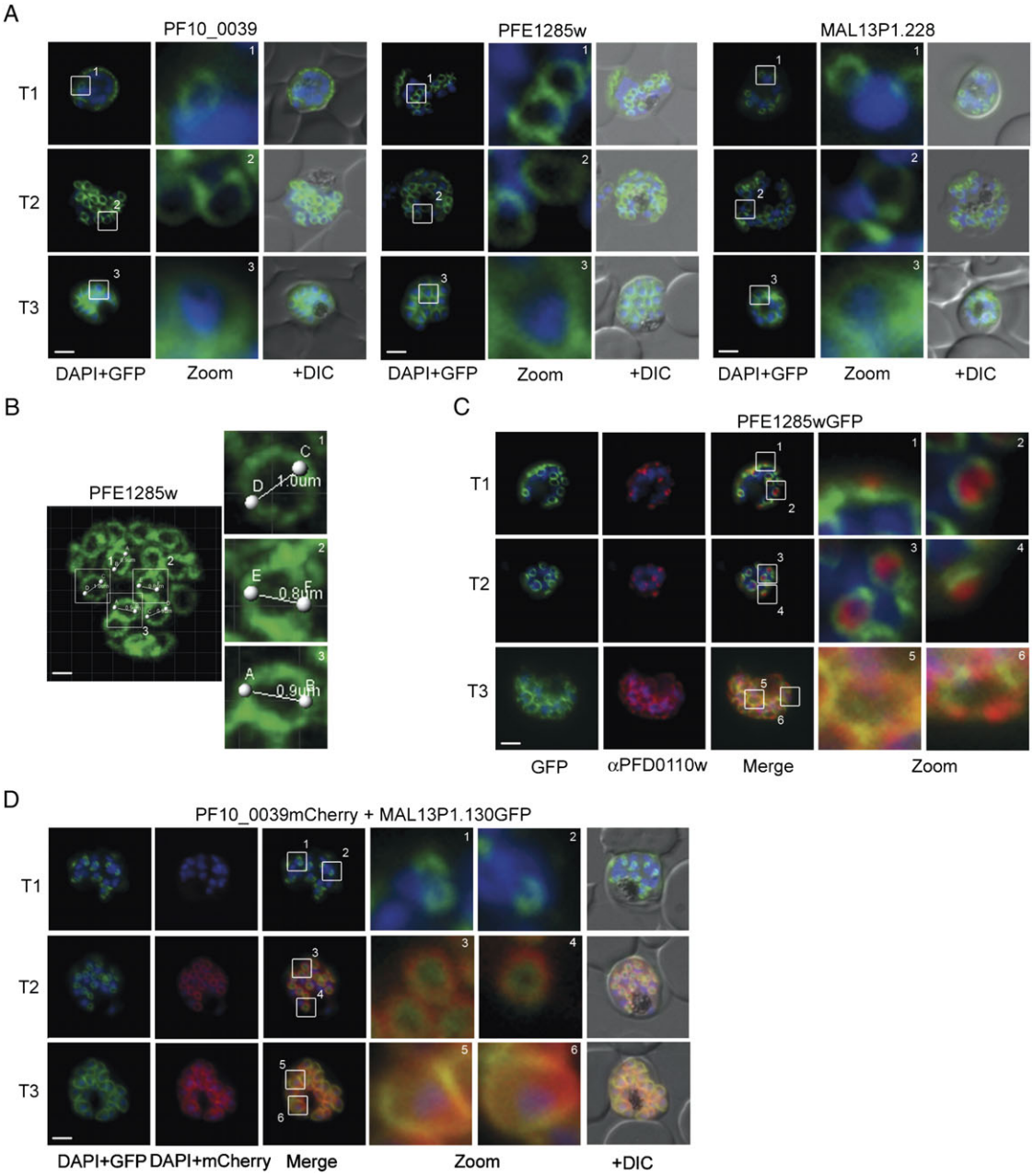

Fig. 4. Group B–associated proteins reveal distinct dynamics. (*A*) The GFP-tagged alveolins PF10_0039, PFE1285w, and the non-alveolin MAL13P1.228 emerge as large ring-like structures (T1-2) that toward the end of schizogony show the same subpellicular distributions as their TMD counterparts (T3). (*B*) The rings have a significant larger diameter (0.9 ± 0.1 μm) compared to group A proteins. (*C*) Colocalization of the group A protein PFD1110w (anti-PFD1110w, red) with the group B alveolin PFE1285w (PFE1285w-GFP, green) emphasizes the differential nature of the two structures in the nascent IMC and their spatial relation during the ongoing schizogony (T1-3). Nuclei stained with DAPI. Scale bars, 1 μm (*B*) and 2 μm (*A*, *C*, and *D*).

separating the two structures highlighted either by group A and B proteins with the group A proteins defining a more distal area in the forming daughter cell (T1 and T2). The spatial separation of the two proteins can be visualized until the development of the forming merozoites is concluded. In this stage, both proteins mark the periphery of the daughter

← 0.63 μm (±0.1 μm) (data shown for MAL13P1.130). (*C* and *D*) Colocalization of the TMD protein MAL13P1.130 and the glideosome-associated protein GAP45. GAP45 was episomally expressed as mCherry-fusion protein and localized in different schizont stages (*C*). Double transgenic cell line expressing MAL13P1.130-GFP and GAP45-mCherry reveals identical spatial distribution (*D*). (*E*) Coexpression of the centrosome marker *Pf*Centrin3-GFP and PF14_0578-mCherry shows a very close association between the forming IMC and the centrosome, as *Pf*Centrin3 marks the center of the developing IMC cramp structure. Nuclei stained with DAPI. Scale bars, 1 μm (*B*) and 2 μm (*A* and *C*–*E*).

cells where the colocalization of the two IMC proteins is almost complete. In a second set of experiments, a double transgenic parasite line was generated expressing a different combination of proteins, MAL13P1.130-GFP (group A) and PF10_0039-mCherry (group B). The dynamic distribution of these two members confirmed the spatial distinction, but intimate proximity of the group A and group B defined IMC subcompartments during the early phase of IMC biogenesis (fig. 4*D*).

Temporal Differences of IMC-Resident Proteins during Schizogony

After validating the spatial differences between these two groups of IMC proteins, their temporal expression patterns were analyzed using one representative of each group.

First, single-cell time-lapse microscopy showed (fig. 5*A* and *B*) that the structure defined by the group A protein can be visualized prior during schizogony (6 ± 1 h before schizont rupture) than the group B–specific structure (4 ± 1 h prior to rupture). The consecutive appearance of the initial structures defined by group A or group B proteins was also investigated by colocalization with the mitotic spindle apparatus (fig. 5*C* and *D*). In agreement with the time-lapse microscopy analysis, the appearance and nucleation of the group B protein was prolonged in comparison with the group A protein and only visible with the disassembly of the spindle apparatus. With ongoing maturation of the schizont and termination of the mitotic segregation, the spindle apparatus is disassembled but remains persistent as perinuclear structures. The distance between the spindle apparatus remnants and the nascent IMC structures appears to be constant with a fixed polarity.

The IMC Defines the Polarity of Nascent Gametocytes

The sexual phase begins with the differentiation of predetermined blood-stage parasites to gametocytes accompanied by profound molecular and morphological changes culminating in mature crescent- or banana-shaped male and female cells about 1.5 times the diameter of a red blood cell in length. Although the molecular machinery for the initiation and differentiation during gametocytogenesis are still largely unknown, the morphologically distinct stages are likely to be reflected in the IMC development during this enigmatic process. First, we used the established gametocyte marker Pfs16 in colocalization with our GFP-fusion proteins PFE1130w, MAL13P1.130, PFD1110w, and PF14_0578 (fig. 6*A*) in gametocyte-enriched transgenic parasite lines. Pfs16 is located in the parasitophorous vacuole membrane and is considered to be one of the earliest known gene products expressed at the onset of gametocytogenesis (Moelans et al. 1991). Almost all IMC proteins tested revealed a restricted localization in early stages of gametocytogenesis, forming a spine-like structure with longitudinal orientation. Three-dimensional reconstruction illustrates the restricted spatial distribution (fig. 6*B* and supplementary movie S5, Supplementary Material online) in these early stages and defines a transversal polarity with the nascent IMC. After establishing the expression of these GFP-tagged proteins in gametocytes, we followed IMC biogenesis throughout all differentiation steps of gametocytes (fig. 6*C*). The round-shaped stage I gametocyte (hardly distinguishable from a pigmented trophozoite) expressing any group A protein is characterized by an elongated GFP-labeled nascent IMC structure that is restricted to one specific side of the cell. This defined flank of the spherical gametocyte is converting into the straight axis of the parasite as it transforms into the characteristic D-shaped stage II from. From here, the defined structure expands congruent with the longitudinal growth of the cell (stage III) and spreads along the inner face of the parasite. In contrast, the distribution of the group B protein MAL13P1.228-GFP fundamentally differs from the group A distribution (fig. 7). Gametocytes expressing MAL13P1.228-GFP reveal distinct lines, which originate from the same structure highlighted by the group A proteins (fig. 7*A* and D). The symmetric lattice is expanding with ongoing maturation (fig. 7*A*) forming a symmetric meshwork enclosing the gametocyte. Three-dimensional reconstruction of a stage II (fig. 7*B* and supplementary movie S6, Supplementary Material online) and stage III (fig. 7*C* and supplementary movie S7, Supplementary Material online) gametocyte emphasizes the spatial distribution of the MAL13P1.228-GFP defined structure and its transversal expansions. Colocalization with the group A protein PFD1110w confirmed not only their differential distribution but also show their synchronized expansion (fig. 7*D* and *E* and supplementary movie S8, Supplementary Material online). Of note, the depicted longitudinal suture shown in figure 6*E* might represent the remnant of the initial spine-like structure highlighted in stage I and II by the group A IMC proteins.

The IMC in Ookinetes and Sporozoites

To extend our investigation of IMC architecture and dynamics into the sporozoite and ookinete stages, we selected a representative from each group for expression in *P. berghei*. The homologs of the group A protein MAL13P1.130 (PB000719.03.0) and group B protein PFE1285w (PB000207.03.0) were cloned and expressed as GFP-fusion proteins. Expression of the fusion protein was driven by 1.5 kB of the endogenous 5′UTR of the two genes. As shown in figure 8*A*, both chimeric proteins revealed a distribution during-blood stage schizogony that was comparable to their *P. falciparum* counterparts. Of note are the differences in size and width of the two types of ring structures.

Subsequently, the distribution of the two proteins was investigated in ookinetes and in liver-stage sporozoites directly at the time point of infection of the HepG2 cells or 2–4 h after infection, respectively. Ookinetes result from preceding mating of gametes and represent the third motile stage during the *Plasmodium* life cycle. Here both proteins appear to be uniformly distributed in the periphery of the protruding ookinetes being absent from the small residual body of the zygote (fig. 8*B* and *B1*,

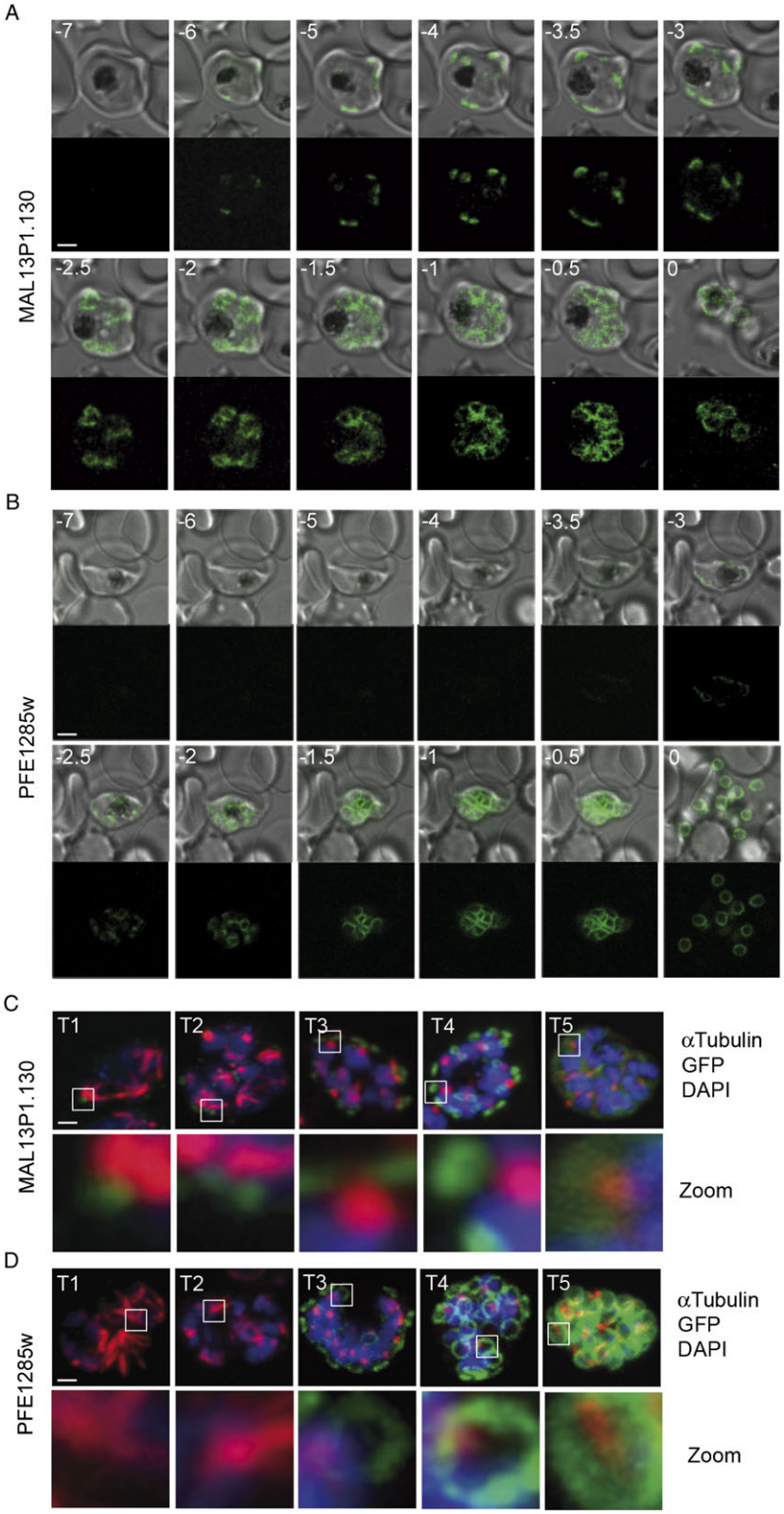

Fig. 5. Temporal relation of IMC proteins during schizogony. (A and *B*) Time-lapse microscopy of individual schizonts expressing the TMD protein MAL13P1.130 (*A*) or the alveolin PFE1285w (*B*) as GFP-fusion proteins. DIC (upper row) or GFP (lower row) time-lapse imaging (intervals indicated upper left corner) of the development of one schizont stage parasites of either MAL13P1.130-GFP or PFE1285w-GFP. Release of merozoites was set to time point zero and counted backward. Size bars, 1 μm. (*C* and *D*) Colocalization of the TMD protein MAL13P1.130 and the alveolin PFE1285w with the disassembling spindle apparatus during schizogony (T1-5). (*C*) Although the mitotic spindles (T1, anti-tubulin, red) are still present, the cramp-like structure highlighted by the TMD protein MAL13P1.130-GFP is formed (T2). (*D*) In contrast, the alveolin-defined structure only emerges after the spindles have retracted forming Microtubule Organization Center bundles (T3). Nuclei stained with DAPI. Scale bars, 2 μm.

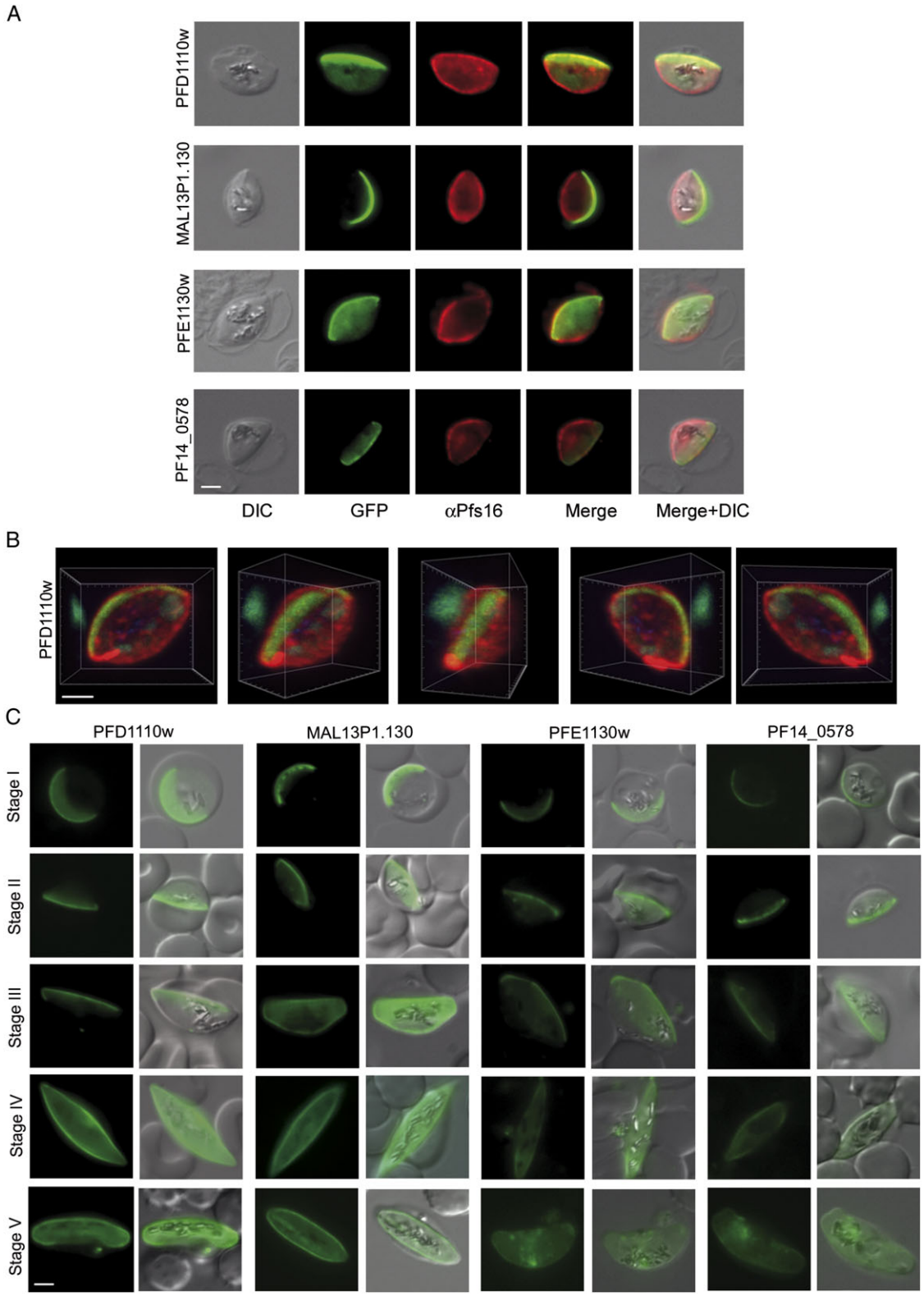

Fig. 6. IMC development during gametocytogenesis. (*A*) Colocalization with the gametocyte marker Pfs16 (α-Pfs16, red) indicates expression and tangential restricted localization of PFE1130w, MAL13P1.130, PFD1110w, and PF14_0578 (green) in early stages of gametogenesis forming a spine-like structure. (*B*) Three-dimensional reconstruction illustrates the spine-like distribution of the IMC (highlighted by PFD1110w-GFP) in forming gametocytes using anti-Pfs16 (red) as a PVM marker. (*C*) IMC dynamic during gametogenesis. The distribution of the TMD proteins as well as PF14_0578 is visualized in all five stages illustrating IMC biogenesis during gamete formation. Scale bars, 2 μm.

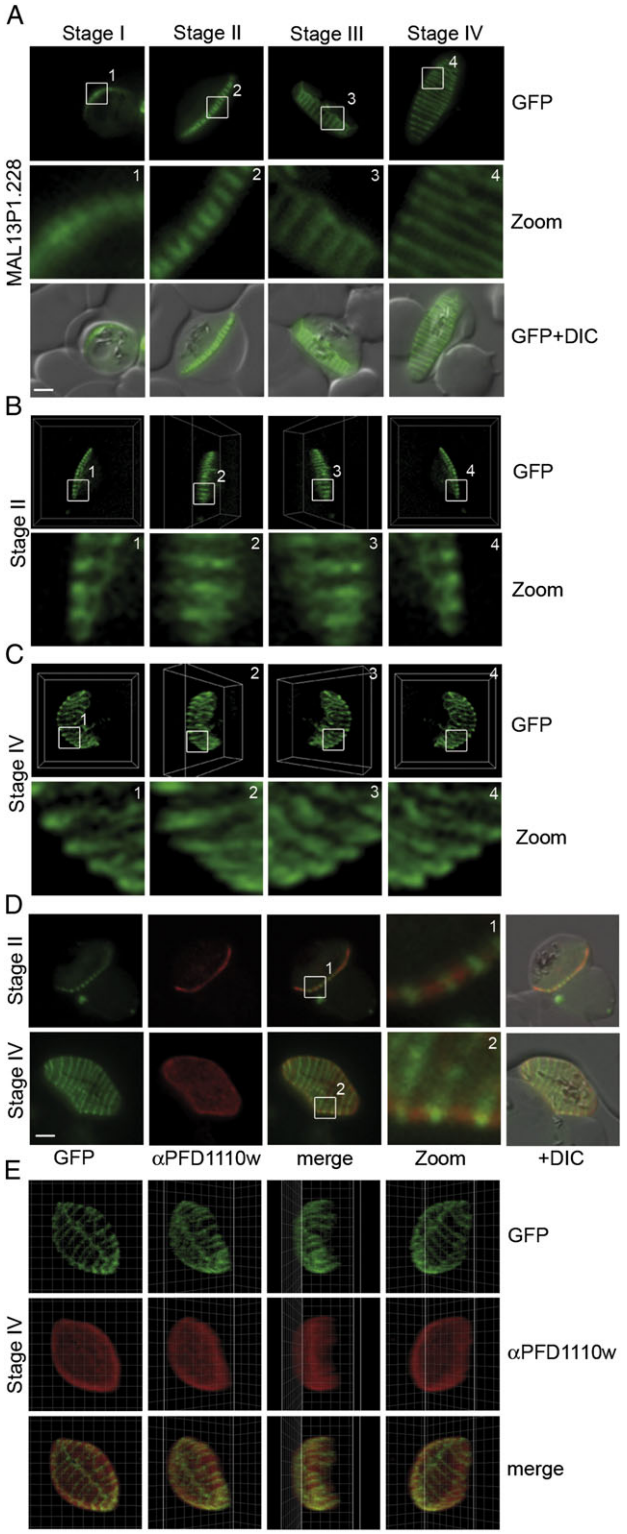

Fig. 7. IMC-resident protein MAL13P1.228 illuminates a novel filamentous meshwork in gametocytes. (*A*) MAL13P1.228-GFP protein highlights sutures that are expanding from a restricted transversal structure in early stage (stage I-II). These symmetric sutures are expanding with ongoing maturation of the gametes (stage III-IV). (*B* and *C*) Three-dimensional reconstruction of a stage II (*B*) and stage IV (*C*) reveal the spatial distribution of MAL13P1.228-GFP during gametogenesis. (*D*) Colocalization of MAL13P1.228 (green) with the TMD protein PFD1110w (red) shows their spatial relation in stage II and stage IV gametocytes (please also refer to the supplementary movies S5 and S6, Supplementary Material online). (*E*) Three-dimensional reconstruction illustrates the differential distribution of MAL13P1.228-GFP and PFD1110w-GFP and their synchronized expansion leads to a progressive encircling of the nascent gametocytes with these IMC components. Scale bars, 2 μm.

B3). This girding localization is continuative in mature ookinetes (fig. 8*B* and *B2*, *B4*), absent only from the apical prominence of the ookinete, where the IMC is associated with the polar rings. These motile forms then traverse the midgut epithelium of the insect to encapsulate under the basal lamina into oocysts. Upon maturation, each oocyst releases several thousand sporozoites into the hemocoel from where they invade the salivary glands. Transgenic sporozoites were isolated from the salivary glands of the mosquitoes and are shown before invasion of the hepatocyte (fig. 8*C1* and *C2*). Both proteins show an even distribution in the periphery of the sporozoites. As expected, the proteins highlighted a peripheral structure and colocalize with the plasma membrane surface marker Circumsporozoite protein since plasma membrane and IMC cannot be distinguished due to their close proximity.

Discussion

Evolution of the IMC Protein Repertoire

One major line of single-cell organisms with a huge impact on mankind are represented by the alveolates, a group that comprises the three phyla: Apicomplexa, Dinoflagellates, and Ciliates (Gajadhar et al. 1991; Cavalier-Smith 1993). Although Alveolata comprises highly diverse classes of eukaryotic cells that adapted to a broad range of ecological niches, they share a common morphological trait termed the IMC that underlies the plasma membrane and is associated with a complex cytoskeletal meshwork (Dubremetz and Torpier 1978; Aikawa et al. 1981; Torpier et al. 1991).

Our phylogenetic analysis reveals that the IMC of *Plasmodium* is composed of a mosaic of proteins of varying evolutionary origin; some are ancient with apparent homologs throughout the eukarya (e.g., PFE1285w and PFE1130w), whereas others are more recent, restricted to the Apicomplexa (e.g., PFF1035w and PF14_0065). Of our 17 initial IMC proteins, only one was *Plasmodium* specific (MAL13P1.228). This is perhaps surprising since ~40% of *Plasmodium* genes are thought to be species specific (Wasmuth et al. 2009) suggesting that many more IMC-associated proteins may yet be identified. Indeed, our analysis identified six additional proteins that may also be associated with IMC and are candidates for future localization studies. Three proteins of the alveolin group (PFC0180c, PFL1030w, and PF10_0039) lack homologs outside the insects and may therefore represent examples of either horizontal gene transfer or convergent evolution. Interestingly, the evolutionary profiles do not correlate with the localization data—within group A, proteins arose at different evolutionary time points. Together these findings support an emerging picture in which many of the components of the IMC evolved

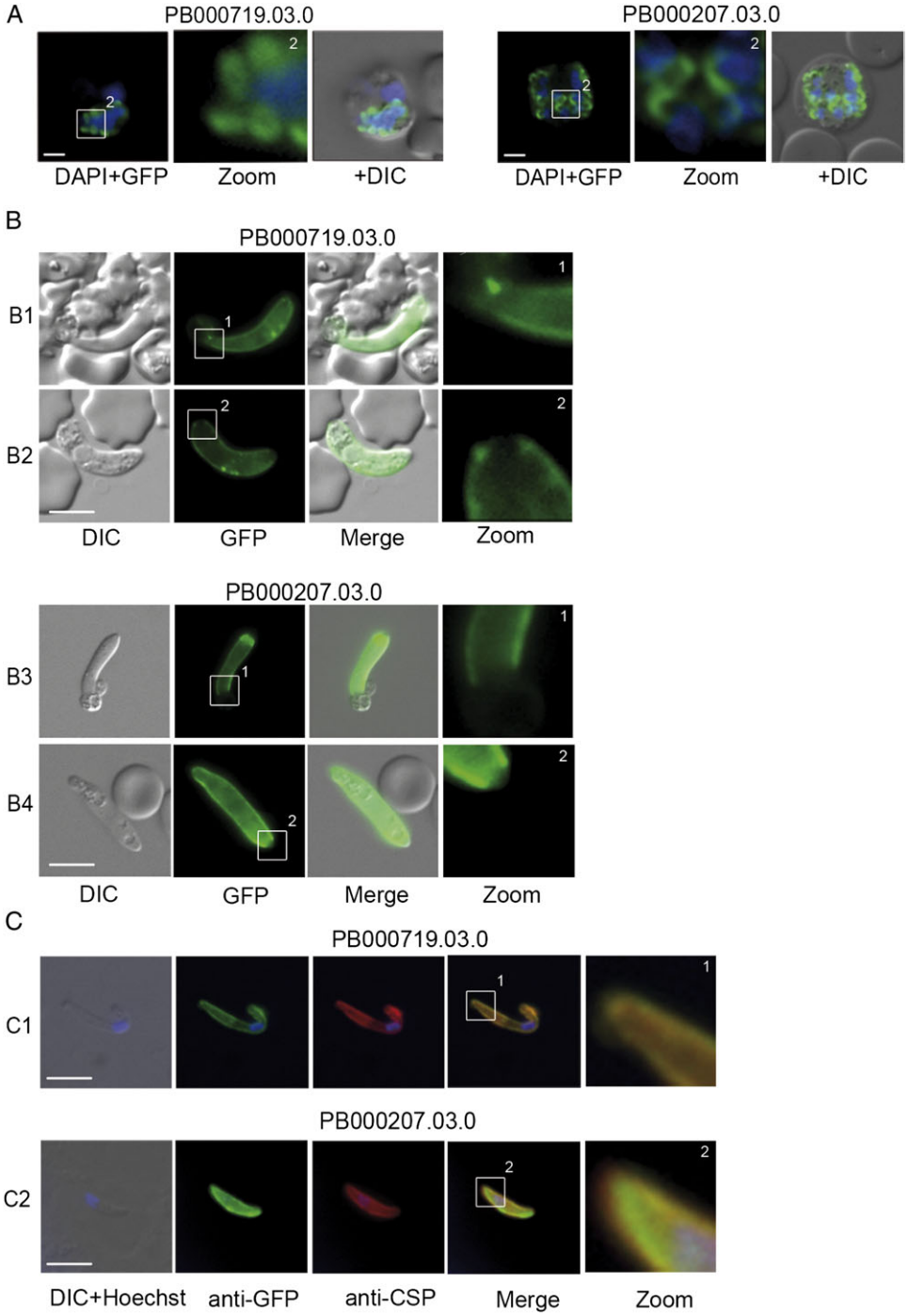

Fig. 8. Localization of a group A and group B protein in *Plasmodium berghei* blood stages, ookinetes, and sporozoites. (*A*) The *P. berghei* orthologs PB000719.03.0 (MAL13P1.130, group A) and PB000207.03.0 (PFE1285w, group B) in blood-stage schizonts reveal similar distribution and dynamic compared with their *P. falciparum* counterparts. (*B*) Both GFP-tagged proteins are uniformly distributed at the IMC in emerging ookinetes (*B*1 and *B*3) as well as in mature ookinetes (*B*2 and *B*4). Of note, some cytosolic background of the proteins can be detected in zygote remnants, and both proteins appear to be absent from the posterior pole of the mature ookinete (fig. *B*1 and *B*3, zoom). (*C*) This peripheral localization can be also visualized in free sporozoites isolated from the salivary glands of the mosquitoes. The parasite plasma membrane is marked with anti-CSP antiserum (red). Scale bars, 2 μm (*A*) and 5 μm (*B* and *C*).

early in the apicomplexan lineage whereas other proteins (PFE1285w, PFE1130w, and PFI0880c) were recruited subsequently to the IMC compartment.

Overall, we note few lineage-specific differences, with clear 1:1 orthologous relationships for many IMC components and species. This suggests that the core IMC machinery emerged relatively early in the apicomplexan lineage and is likely functionally conserved across the phylum. However, there are several notable exceptions. For example relative to the other Apicomplexa, Theileria appears to lack orthologs of several alveolins including PFL1030w, PF14_0168, and PFF1035. In addition, the absence of an identifiable homolog

of PFE1130w suggests that the IMC machinery may be organized and operate differently within this lineage. Similarly, the presence of duplicate copies of the six-transmembrane proteins: PFD1110w and MAL13P1.130 in *T. gondii* may represent lineage-specific innovations perhaps required for its unique invasion strategies. Future studies are needed to investigate whether the paralogs in these species provide "backup" compensatory functions or provide novel and/or distinct functionality that arose through a process of neo- or subfunctionalization process (He and Zhang 2005).

Subcompartmentalization and Architecture in Asexual Stages

Earlier ultrastructural work performed on *Tetrahymena thermophila* (Satir and Wissig 1982) and apicomplexan parasites like *Eimeria* sp. sporozoites (Dubremetz and Torpier 1978), *T. gondii* tachyzoites (Morrissette et al. 1997), and *P. falciparum* gametocytes (Meszoely et al. 1987) already revealed the complexity of the pellicle and the diversity of its composition in different alveolate organisms. Although in most cases, the IMC is built of several flattened and elongated vesicles that are joined by sutures clearly visible in electron microscopy analyses (Dubremetz and Torpier 1978), only a single vesicle is reported for *Plasmodium* merozoites (Bannsiter and Mitchell 1995). Recent studies initiated the dissection of the molecular basis of IMC subcompartmentalization mainly in *T. gondii*. An astonishing diversity in the spatiotemporal distribution of IMC proteins even within a family of proteins was observed (Anderson-White et al. 2011). Considerably less is known for the malaria parasite. Most of the studies focused on the IMC dynamic during blood-stage development using either six-transmembrane domain proteins (Bullen et al. 2009; Rayavara et al. 2009; Hu et al. 2010), GAP45 (Rees-Channer et al. 2006; Green et al. 2008; Jones et al. 2009; Frénal et al. 2010), or GAP50 (Yeoman et al. 2011). In all these studies, the reviewed proteins revealed the same dynamic in nascent as well as in mature merozoites. We further extended the former studies by using a broader variety of structurally and phylogenetically distinct IMC proteins and initiated a detailed characterization of this compartment in other zoites and nonmotile forms. First, we showed that the previously described dynamics (Bullen et al. 2009) are also mirrored by PFE1130w (a novel seven-transmembrane domain protein) and the N-terminally acylated protein PF14_0578. The latter one shows 12–18% identity to *Pf*GAP45 and the *T. gondii* protein IMC Subcompartment Protein 1 (ISP1) (Beck et al. 2010), respectively. Simultaneous labeling of MAL13P1.130 with the established IMC protein GAP45 showed an identical protein distribution during IMC formation. Of note, MAL13P1.130 and PFD1110w were previously copurified with the actin–myosin motor including GAP45 itself and therefore termed *g*lideosome-*a*ssociated *p*rotein with multiple-*m*embrane spans (GAPM, Bullen et al. 2009). Coincidently, PFE1130w and PF14_0578 share the same phenotype clearly distinguishing themselves from the group B proteins, which might point toward a glideosome-associated function. Further interaction studies are needed to investigate these findings.

Since nascent IMC structures, that are labeled by group A proteins, can already be visualized in young schizonts, we wanted to determine their association with the centrosome and a possible role of the IMC in the early processes of cytokinesis such as scaffolding as it was described for *T. gondii* (Hu 2008; Agop-Nersesian et al. 2009). We used the centrosome-associated protein *Pf*Centrin3. Previous work suggested that the centrosome might be involved in initiating the budding of daughter cells and organizing the developing apical organelles (Mahajan et al. 2008). The intimate spatial and temporal association of the centrosome with the nascent IMC visualized by group A proteins (fig. 3*E*) might be indicative for either a direct or indirect role of the centrosome in the very early stages of IMC biogenesis. This idea is consistent with a previous study in *T. gondii* suggesting that the entire daughter cell is built around the centriole by adapting this structure as a "master organizer" (Striepen et al. 2000).

The group B proteins are only visible when the ring structures highlighted by group A proteins are already established. In addition to the later appearance shown by time-lapse microscopy, these proteins label only the proximal rim of the rings and therefore appear as bigger hoops surrounding the smaller protein A defined structures. The clear spatial and temporal separation of the initial structure of group A and B proteins argues for a putative subcompartmentalization of the (nascent) IMC. This would be reminiscent of the *T. gondii* IMC organization, where various IMC-resident proteins have not only different time points of appearance but also distinct localization patterns in the newly formed IMC of daughter cells (Beck et al. 2010; Anderson-White et al. 2011). The consecutive appearance of the group A and group B structures implies that the assembly of the later depends on the initiation of the first, leading to a successive construction of the IMC and representing coordinated steps during daughter cell assembly. Interestingly, group A and B proteins also differ in their mode of membrane attachment.

IMC Membrane Association

IMC membrane association is mediated by multiple means. Signal peptide containing transmembrane spanning proteins like PFE1130w as well as their six-transmembrane counterparts (MAL13P1.130 and PFD1110w) are likely to use the vesicle-mediated transport mechanism of secretory proteins to get delivered to the membrane of the IMC as previously suggested (Raibaud et al. 2001; Yeoman et al. 2011). In contrast, PF14_0578 uses N-terminal lipid modifications as IMC membrane attachment moieties (Gilberger laboratory, unpublished data). This was also established for the ISP proteins in *T. gondii* where membrane specificity was explained by a kinetic trapping model: proteins are cotranslationally myristoylated in the cytosol, enabling reversible membrane attachment. Consequently, they are recognized and palmitoylated by a unique palmitoyl acyltransferase (PAT) that is present at the IMC and

exclusively recognizes these proteins (Beck et al. 2010). This could be a likely scenario for the malaria parasite as well given that some of the 12 PATs encoded in the malaria genome are cotranscriptionally upregulated with the IMC proteins (Bozdech et al. 2003) and are predicted to be involved in invasion (Hu et al. 2010).

Specific IMC membrane recruitment strategies for the group B proteins, including the two alveolins used in this study, and MAL13P1.228 appear to be less clear. Interestingly, all these proteins nucleate at the ring structure toward the apical end before they get distributed along the periphery of the nascent parasites. A mutational analysis of the two alveolins in *T. gondii* (IMC3 and IMC8), both without any acylation motifs, showed that the alveolin repeats were sufficient for IMC localization (Anderson-White et al. 2011). MAL13P1.228 does not contain any alveolin repeat or any other recognizable structural motifs such as amphipathic helices that could mediate hydrophobic interactions facilitating membrane association (Ossorio et al. 1994; Picot et al. 1994). We hypothesize that MAL13P1.228 is specifically recruited to its destination through specific protein–protein interactions, similar to the well-established interactions observed for instance in peripheral Golgi membrane proteins (Ramirez and Lowe 2009). This is reminiscent of Phil1 (photosensitized 5-[125I]iodonaphthalene-1-azide-labeled protein 1) that without any recognizable transmembrane domains or lipid modification motifs and deleted amphipathic helix and N-terminus, still localize to the peripheral membrane system (Gilk et al. 2006).

IMC Architecture in Gametocytes

Although the function of the IMC for motility has generated considerable interest, its function during gametocytogenesis is not yet established. It can be assumed that the primary function of the IMC lies in scaffolding and maintaining cell shape based on the mechanical strength of its complex structures (Mann and Beckers 2001). Gametocytogenesis involves the transformation of an almost spherical cell with a diameter of ~3 to 4 μm into a ~9 μm crescent-shaped stage V gametocyte that is ready for uptake by the mosquito. The first ultrastructural evidence of the transformation from stage I to II gametocyte is the de novo formation of a "subpellicular membrane vesicle or complex" together with an array of microtubules (Sinden 1982, 1983). We used our set of GFP-tagged IMC proteins to investigate the developmental process of this compartment and proof the congeneric nature of the IMC in merozoites and gametocytes. All group A proteins nucleated at an elongated structure that defines the transversal polarity in the first stages of gametocytogenesis. Hence, these findings complement earlier ultrastructural work that showed that the developing IMC defines the polarity of the cell through determining the straight side of the stage II gametocyte (Sinden 1982). From here, the compartment first lengthens retransforming the cell into its characteristic D-form and then enlarges simultaneously with further growth of the parasite. Although the group A proteins are homogeneously distributed through the elongated IMC structure, MAL13P1.228 (an apparent *Plasmodium* innovation) is located in restricted areas resulting first in a punctuated and later stripy appearances. Both alveolins (PF10_0039 and PFE1285w) revealed only a weak fluorescence that did not allow a more detailed microscopic analysis. The characteristic localization of MAL13P1.228-GFP is reminiscent of structures described in ultrastructural analysis performed by Meszoely et al. (1987) using freeze fractures of *P. falciparum* gametocytes. They reported a series of transverse sutures on the gametocyte middle membrane that subdivides several ring-like plates giving the parasite a segmented appearance. They suggested that these sutures might be implicated in some special affinity between the plasma membrane and outer membrane of the IMC. Although Meszoely et al. (1987) observed only up to 11 of these transverse sutures and we observe an average of 13 (±3) for each gametocyte, we hypothesize that MAL13P1.228 is one molecular marker of these sutures. This is supported by the dynamic of MAL13P1.228 and its restricted localization to the transversal structures. Interestingly, a concurrent study focusing on *Pf*GAP50 localization in gametocytes using electron microscopy and Structured Illumination Microscopy (SIM) revealed fine-spun "stripy" distribution of this protein. The authors argue that the GAP50 distribution might visualize the IMC cisternae laid down as rectangular plates, while the gaps represent the proteinaceous material that holds the cisternae and the microtubules in place (Dearnley M, Dixon M, personal communication). This architecture might be important to address the structural needs of the developing gametocyte by enhancing the physical strength and assuring deformability of the cell by partitioning of the pellicle. Coincidentally, MAL13P1.228 appears to be a *Plasmodium*-specific innovation, indicating a unique function of the IMC within the genus.

IMC Development in Ookinetes and Sporozoites

We extended our comparative analysis of group A and B proteins to sporozoites and ookinetes and localized the *P. berghei* homolog of the group A protein MAL13P1.130 (PB000719.03.0) and the group B protein PFE1285w (PB000207.03.0) in both stages. We showed that both proteins localize to the periphery of the parasite and are therefore most likely part of the pellicle of both stages as their *P. falciparum* counterparts. The phenotype is consistent with previous work, where IMC proteins IMC a, b and IMC h showed similar localization patterns in sporozoites and ookinetes (Khater et al. 2004; Tremp et al. 2008). The available expression data of the two selected homologues (PFE1285w/PB000207.03.0 and MAL13P1.130/PB000719.03.0) indicated expression in all stages, different from previous studies that focus on IMC-associated proteins with a restricted expression profile in sporozoites and ookinetes (PbIMC1a, Khater et al. 2004; PbIMC1h, Tremp et al. 2008; and PbIMC1b, Tremp and Dessens 2011). Although our data in *P. berghei* blood stages show noticeable differences that are reminiscent of the described differential dynamics and subcompartmentalization of the *P. falciparum*

homologs, we could not detect any differential localization of the two proteins in sporozoites or ookinetes. This might be due to technical limitations in this initial study and the absence of time-lapse microscopy but could also illustrate profound differences in the IMC architecture between the nonmotile and motile stages.

In summary, conservation of the IMC as a subcellular structure in various organisms with diverse lifestyles throughout the entire alveolate super group is testament for its versatile utility. We revealed a plethora of structural organization and phylogenetic trajectories of *Plasmodium* IMC proteins that exemplifies the adaptive molecular composition of the IMC with a subset of core proteins that are highly conserved. Further analysis of the complexity of the IMC proteins composition in various genera from the Alveolata in combination with the functional analysis of individual proteins will provide us with a detailed insight into the evolutionary forces acting on this synmorphic structure that is ancient, adaptable, and multifunctional.

Supplementary Material

Supplementary table 1, figures 1–8, text 1, and movies S1–S8 are available at *Molecular Biology and Evolution* online (http://www.mbe.oxfordjournals.org/).

Acknowledgments

We would like to thank Pietro Alano for anti-Pfs16 and to Jacobus Pharmaceuticals for providing WR99210. This study was supported by grants from the Deutsche Forschungsgemeinschaft (GRK# 1549) and Canadian Institutes for Health Research (MOP# 111196 to T.W.G. and MOP# 84556 to J.P.). We thank Dr Mary J. O'Connell and the Bioinformatics and Molecular Evolution group, Dublin City University for the use of their computational facilities.

References

Agop-Nersesian C, Naissant B, Ben Rached F, Rauch M, Kretzschmar A, Thiberge S, Menard R, Ferguson F, Meissner M, Langsley G. 2009. Rab11A-controlled assembly of the inner membrane complex is required for completion of apicomplexan cytokinesis. *PLoS Pathog.* 5:e1000270.

Aikawa M, Miller L, Rabbege J, Epstein N. 1981. Freeze-fracture study on the erythrocyte membrane during malarial parasite invasion. *J Cell Biol.* 91:55–62.

Allen RD. 1971. Fine structure of membranous and microfibrillar systems in the cortex of Paramecium caudatum. *J Cell Biol.* 49:1–20.

Anderson-White B, Ivey F, Cheng K, Szatanek T, Lorestani A, Beckers C, Ferguson D, Sahoo N, Gubbels M. 2011. A family of intermediate filament-like proteins is sequentially assembled into the cytoskeleton of *Toxoplasma gondii*. *Cell Microbiol.* 13:18–31.

Bannister LH, Mitchell GH. 1995. The role of the cytoskeleton in Plasmodium falciparum merozoite biology: an electron-microscopic view. *Ann TRop Med Parasitol.* 89:105–111.

Baum J, Gilberger T, Frischknecht F, Meissner M. 2008. Host-cell invasion by malaria parasites: insights from *Plasmodium* and *Toxoplasma*. *Trends Parasitol.* 24:557–563.

Baum J, Richard D, Healer J, Rug M, Krnajski Z, Gilberger T, Green J, Holder A, Cowman A. 2006. A conserved molecular motor drives cell invasion and gliding motility across malaria life cycle stages and other apicomplexan parasites. *J Biol Chem.* 281: 5197–5208.

Beck J, Rodriguez-Fernandez I, Cruz de Leon J, Huynh M, Carruthers V, Morrissette N, Bradley P. 2010. A novel family of Toxoplasma IMC proteins displays a hierarchical organization and functions in coordinating parasite division. *PLoS Pathog.* 6:e1001094.

Berglund A, Sjolund E, Ostlund G, Sonnhammer E. 2008. InParanoid 6: eukaryotic ortholog clusters with inparalogs. *Nucleic Acids Res.* 36:D263–D266.

Bergman L, Kaiser W, Fujioka H, Coppens I, Daly T, Fox S, Matuschewski K, Nussenzweig V, Kappe S. 2003. Myosin A tail domain interacting protein (MTIP) localizes to the inner membrane complex of *Plasmodium* sporozoites. *J Cell Sci.* 116: 39–49.

Bosch J, Turley S, Roach CM, Daly TM, Bergman LW, Hol WG. 2007. The closed MTIP-myosin A-tail complex from the malaria parasite invasion machinery. *J Mol Biol.* 372:77–88.

Bozdech Z, Llinas M, Pulliam B, Wong E, Zhu J, DeRisi JL. 2003. The transcriptome of the intraerythrocytic developmental cycle of *Plasmodium falciparum*. *PLoS Biol.* 1:E5.

Bullen H, Tonkin C, O'Donnell R, Tham W, Papenfuss A, Gould S, Cowman A, Crabb B, Gilson P. 2009. A novel family of Apicomplexan glideosome-associated proteins with an inner membrane-anchoring role. *J Biol Chem.* 284:25353–25363.

Capella-Gutierrez S, Silla-Martinez JM, Gabaldon T. 2009. trimAl: a tool for automated alignment trimming in large-scale phylogenetic analyses. *Bioinformatics* 25:1972–1973.

Cavalier-Smith T. 1993. Kingdom protozoa and its 18 phyla. *Microbiol Rev.* 57:953–994.

Chen F, Mackey AJ, Stoeckert CJ Jr, Roos DS. 2006. OrthoMCL-DB: querying a comprehensive multi-species collection of ortholog groups. *Nucleic Acids Res.* 34(Database issue): D363–D368.

Daher W, Pierrot C, Kalamou H, Pinder JC, Margos G, Dive D, Franke-Fayard B, Janse CJ, Khalife J. 2010. Plasmodium falciparum dynein light chain 1 interacts with actin/myosin during blood stage development. *J Biol Chem.* 285:20180–20191.

de Miguel N, Lebrun M, Heaslip A, Hu K, Beckers C, Matrajt M, Dubremetz J, Angel S. 2008. *Toxoplasma gondii* Hsp20 is a stripe-arranged chaperone-like protein associated with the outer leaflet of the inner membrane complex. *Biol Cell.* 100:479–489.

Dubremetz J, Torpier G. 1978. Freeze fracture study of the pellicle of an eimerian sporozoite (Protozoa, Coccidia). *J Ultrastruct Res.* 62:94–109.

Eddy S. 2009. A new generation of homology search tools based on probabilistic inference. *Genome Inform.* 23:205–211.

Edgar R. 2004. MUSCLE: a multiple sequence alignment method with reduced time and space complexity. *BMC Bioinformatics* 5:113.

Ferguson DJ, Sahoo N, Pinches RA, Bumstead JM, Tomley FM, Gubbels MJ. 2008. MORN1 has a conserved role in asexual and sexual development across the apicomplexa. *Eukaryot Cell.* 7:698–711.

Fidock D, Wellems T. 1997. Transformation with human dihydrofolate reductase renders malaria parasites insensitive to WR99210 but does not affect the intrinsic activity of proguanil. *Proc Natl Acad Sci U S A.* 94:10931–10936.

Fivelman Q, McRobert L, Sharp S, Taylor C, Saeed M, Swales C, Sutherland C, Baker D. 2007. Improved synchronous production of *Plasmodium falciparum* gametocytes in vitro. *Mol Biochem Parasitol.* 154:119–123.

Flicek P, Amode R, Barrell D, et al. 2011. Ensembl 2011. *Nucleic Acids Res.* 39:D800–D806.

Flueck C, Bartfai R, Niederwieser I, Witmer K, Alako B, Moes S, Bozdech Z, Jenoe P, Stunnenberg H, Voss T. 2010. A major role for the Plasmodium falciparum ApiAP2 protein PfSIP2 in chromosome end biology. *PLoS Pathog.* 6:e1000784.

Frénal K, Polonais V, Marq J, Stratmann R, Limenitakis J, Soldati-Favre D. 2010. Functional dissection of the apicomplexan glideosome molecular architecture. *Cell Host Microbe.* 8:343–357.

Gajadhar A, Marquardt W, Hall R, Gunderson J, Ariztia-Carmona E, Sogin M. 1991. Ribosomal RNA sequences of *Sarcocystis muris, Theileria annulata* and *Crypthecodinium cohnii* reveal evolutionary relationships among apicomplexans, dinoflagellates, and ciliates. *Mol Biochem Parasitol.* 45:147–154.

Gaskins E, Gilk S, DeVore N, Mann T, Ward G, Beckers C. 2004. Identification of the membrane receptor of a class XIV myosin in *Toxoplasma gondii*. *J Cell Biol.* 165:383–393.

Gilk S, Raviv Y, Hu K, Murray J, Beckers C, Ward G. 2006. Identification of PhIL1, a novel cytoskeletal protein of the *Toxoplasma gondii* pellicle, through photosensitized labeling with 5-[125I]iodonaphthalene-1-azide. *Eukaryot Cell.* 5:1622–1634.

Gould S, Kraft L, van Dooren G, Goodman C, Ford K, Cassin A, Bacic A, McFadden G, Waller R. 2011. Ciliate pellicular proteome identifies novel protein families with characteristic repeat motifs that are common to alveolates. *Mol Biol Evol.* 28:1319–1331.

Gould S, Tham W, Cowman A, McFadden G, Waller R. 2008. Alveolins, a new family of cortical proteins that define the protist infrakingdom Alveolata. *Mol Biol Evol.* 25:1219–1230.

Green JL, Martin SR, Fielden J, Ksagoni A, Grainger M, Yim Lim BY, Molloy JE, Holder AA. 2006. The MTIP-myosin A complex in blood stage malaria parasites. *J Mol Biol.* 355:933–941.

Green J, Rees-Channer R, Howell S, Martin S, Knuepfer E, Taylor H, Grainger M, Holder A. 2008. The motor complex of *Plasmodium falciparum*: phosphorylation by a calcium-dependent protein kinase. *J Biol Chem.* 283:30980–30989.

Grüring C, Heiber A, Kruse F, Ungefehr J, Gilberger T, Spielmann T. 2011. Development and host cell modifications of *Plasmodium falciparum* blood stages in four dimensions. *Nat Commun.* 2:165.

Gubbels M, Wieffer M, Striepen B. 2004. Fluorescent protein tagging in *Toxoplasma gondii*: identification of a novel inner membrane complex component conserved among Apicomplexa. *Mol Biochem Parasitol.* 137:99–110.

Guindon S, Gascuel O. 2003. A simple, fast, and accurate algorithm to estimate large phylogenies by maximum likelihood. *Syst Biol.* 52:696–704.

He X, Zhang J. 2005. Rapid subfunctionalization accompanied by prolonged and substantial neofunctionalization in duplicate gene evolution. *Genetics* 169:1157–1164.

Hu K. 2008. Organizational changes of the daughter basal complex during the parasite replication of *Toxoplasma gondii*. *PLoS Pathog.* 4:e10.

Hu G, Cabrera A, Kono M, et al. (12 co-authors). 2010. Transcriptional profiling of growth perturbations of the human malaria parasite *Plasmodium falciparum*. *Nat Biotechnol.* 28:91–98.

Huang Y, Niu B, Gao Y, Fu L, Li W. 2010. CD-HIT Suite: a web server for clustering and comparing biological sequences. *Bioinformatics* 26:680–682.

Janse C, Ramesar J, Waters A. 2006. High-efficiency transfection and drug selection of genetically transformed blood stages of the rodent malaria parasite *Plasmodium berghei*. *Nat Protoc.* 1:346–356.

Jones ML, Kitson EL, Rayner JC. 2006. Plasmodium falciparum erythrocyte invasion: a conserved myosin associated complex. *Mol Biochem Parasitol.* 147:74–84.

Jones M, Cottingham C, Rayner J. 2009. Effects of calcium signaling on *Plasmodium falciparum* erythrocyte invasion and post-translational modification of gliding-associated protein 45 (PfGAP45). *Mol Biochem Parasitol.* 168:55–62.

Keane T, Creevey C, Pentony M, Naughton T, McLnerney J. 2006. Assessment of methods for amino acid matrix selection and their use on empirical data shows that ad hoc assumptions for choice of matrix are not justified. *BMC Evol Biol.* 6:29.

Keeley A, Soldati D. 2004. The glideosome: a molecular machine powering motility and host-cell invasion by Apicomplexa. *Trends Cell Biol.* 14:528–532.

Khater E, Sinden R, Dessens J. 2004. A malaria membrane skeletal protein is essential for normal morphogenesis, motility, and infectivity of sporozoites. *J Cell Biol.* 167:425–432.

Lee RE, Kugrens P. 1992. Relationship between the flagellates and ciliates. *Microbiol Rev.* 56:529–542.

Li L, Stoeckert CJ, Roos DS. 2003. OrthoMCL: identification of ortholog groups for eukaryotic genomes. *Genome Res.* 13:2178–2189.

Lorestani A, Sheiner L, Yang K, Robertson S, Sahoo N, Brooks C, Ferguson D, Striepen B, Gubbels M. 2010. A *Toxoplasma* MORN1 null mutant undergoes repeated divisions but is defective in basal assembly, apicoplast division and cytokinesis. *PLoS One* 19:e12302.

Mahajan B, Selvapandiyan A, Gerald N, et al. (12 co-authors). 2008. Centrins, cell cycle regulation proteins in human malaria parasite *Plasmodium falciparum*. *J Biol Chem.* 283:31871–31883.

Mann T, Beckers C. 2001. Characterization of the subpellicular network, a filamentous membrane skeletal component in the parasite *Toxoplasma gondii*. *Mol Biochem Parasitol.* 115:257–268.

Meszoely C, Erbe E, Steere R, Trosper J, Beaudoin RL. 1987. *Plasmodium falciparum*: freeze-fracture of the gametocyte pellicular complex. *Exp Parasitol.* 64:300–309.

Moelans I, Klaassen C, Kaslow D, Konings R, Schoenmakers J. 1991. Minimal variation in Pfs16, a novel protein located in the membrane of gametes and sporozoites of *Plasmodium falciparum*. *Mol Biochem Parasitol.* 46:311–313.

Morrissette N, Murray J, Roos D. 1997. Subpellicular microtubules associate with an intramembranous particle lattice in the protozoan parasite *Toxoplasma gondii*. *J Cell Sci.* 110:35–42.

Morrissette N, Sibley D. 2002. Cytoskeleton of apicomplexan parasites. *Microbiol Mol Biol Rev.* 66:21–38.

O'Brien K, Remm M, Sonnhammer E. 2005. Inparanoid: a comprehensive database of eukaryotic orthologs. *Nucleic Acids Res.* 33:D476–D480.

On T, Xiong X, Pu S, Turinsky A, Gong Y, Emili A, Zhang Z, Greenblatt J, Wodak SJ, Parkinson J. 2010. The evolutionary landscape of the chromatin modification machinery reveals lineage specific gains, expansions, and losses. *Proteins* 78:2075–2089.

Ossorio P, Dubremetz J, Joiner K. 1994. A soluble secretory protein of the intracellular parasite *Toxoplasma gondii* associates with the parasitophorous vacuole membrane through hydrophobic interactions. *J Biol Chem.* 269:15350–15357.

Ota R, Waddell P, Hasegawa M, Shimodaira H, Kishino H. 2000. Appropriate likelihood ratio tests and marginal distributions for evolutionary tree models with constraints on parameters. *Mol Biol Evol.* 17:798–803.

Peregrin-Alvarez J, Yam J, Sivakumar G, Parkinson J. 2005. PartiGeneDB—collating partial genomes. *Nucleic Acids Res.* 33:D303–D307.

Picot S, Sheick I, Sylvi A, Donadille A, Ambroise-Thomas P. 1994. Signal transduction pathways involved in tumour necrosis factor secretion by *Plasmodium falciparum*-stimulated human monocytes. *Immunology* 83:70–74.

Raibaud A, Lupetti P, Paul R, Mercati D, Brey P, Sinden R, Heuser J, Dallai R. 2001. Cryofracture electron microscopy of the ookinete

pellicle of *Plasmodium gallinaceum* reveals the existence of novel pores in the alveolar membranes. *J Struct Biol.* 135:47–57.
Rambaut A, Grassly N, Nee S, Harvey P. 1996. Bi-De: an application for simulating phylogenetic processes. *Comput Appl Biosci.* 12:469–471.
Ramirez I, Lowe M. 2009. Golgins and GRASPs: holding the Golgi together. *Semin Cell Dev Biol.* 20:770–779.
Rayavara K, Rajapandi T, Wollenberg K, Kabat J, Fischer E, Desai S. 2009. A complex of three related membrane proteins is conserved on malarial merozoites. *Mol Biochem Parasitol.* 167:135–143.
Rees-Channer R, Martin S, Green J, Bowyer P, Grainger M, Molloy J, Holder A. 2006. Dual acylation of the 45 kDa gliding-associated protein (GAP45) in *Plasmodium falciparum* merozoites. *Mol Biochem Parasitol.* 149:113–116.
Remm M, Storm C, Sonnhammer E. 2001. Automatic clustering of orthologs and in-paralogs from pairwise species comparisons. *J Mol Biol.* 314:1041–1052.
Ronquist F, Huelsenbeck JP. 2003. MrBayes 3: Bayesian phylogenetic inference under mixed models. *Bioinformatics* 19:1572–1574.
Sanders PR, Gilson PR, Cantin GT, et al. (11 co-authors). 2005. Distinct protein classes including novel merozoite surface antigens in Raft-like membranes of *Plasmodium falciparum*. *J Biol Chem.* 280:40169–40176.
Sanders PR, Cantin GT, Greenbaum DC, Gilson PR, Nebl T, Moritz RL, Yates JR III, Hodder AN, Crabb BS. 2007. Identification of protein complexes in detergent-resistant membranes of *Plasmodium falciparum* schizonts. *Mol Biochem Parasitol.* 154: 148–157.
Satir B, Wissig S. 1982. Alveolar sacs of *Tetrahymena*: ultrastructural characteristics and similarities to subsurface cisterns of muscle and nerve. *J Cell Sci.* 55:13–33.
Schmidt H, Strimmer K, Vingron M, von Haeseler A. 2002. TREE-PUZZLE: maximum likelihood phylogenetic analysis using quartets and parallel computing. *Bioinformatics* 18:502–504.
Shannon P, Markiel A, Ozier O, Baliga N, Wang J, Ramage D, Amin N, Schwikowski B, Ideker T. 2003. Cytoscape: a software environment for integrated models of biomolecular interaction networks. *Genome Res.* 13:2498–2504.
Sinden R. 1982. Gametocytogenesis of *Plasmodium falciparum* in vitro: an electron microscopic study. *Parasitology* 84:1–11.
Sinden R. 1983. Sexual development of malarial parasites. *Adv Parsitol.* 22:153–216.
Soldati D, Foth B, Cowman A. 2004. Molecular and functional aspects of parasite invasion. *Trends Parasitol.* 20:567–574.
Striepen B, Crawford MJ, Shaw MK, Tilney LG, Seeber F, Roos DS. 2000. The plastid of *Toxoplasma gondii* is divided by association with the centrosomes. *J Cell Biol.* 151:1423–1434.
Struck N, de Souza S, Langer C, Marti M, Pearce J, Cowman A, Gilberger T. 2005. Re-defining the Golgi complex in *Plasmodium falciparum* using the novel Golgi marker PfGRASP. *J Cell Sci.* 118:5603–5613.
Thomas JC, Green JL, Howson RI, Simpson P, Moss DK, Martin SR, Holder AA, Cota E, Tate EW. 2010. Interaction and dynamics of the *Plasmodium falciparum* MTIP-MyoA complex, a key component of the invasion motor in the malaria parasite. *Mol Biosyst.* 6:494–498.
Tonkin C, van Dooren G, Spurck T, Struck N, Good R, Handman E, Cowman A, McFadden G. 2004. Localization of organellar proteins in *Plasmodium falciparum* using a novel set of transfection vectors and a new immunofluorescence fixation method. *Mol Biochem Parasitol.* 137:13–21.
Torpier G, Darde M, Caron H, Darcy F, Capron A. 1991. *Toxoplasma gondii*: membrane structure differences between zoites demonstrated by freeze fracture analysis. *Exp Parasitol.* 72:99–102.
Trager W, Jensen J. 1976. Human malaria parasites in continuous culture. *Science* 193:673–675.
Treeck M, Struck NS, Haase S, Langer C, Herrmann S, Healer J, Cowman AF, Gilberger TW. 2006. A conserved region in the EBL proteins is implicated in microneme targeting of the malaria parasite *Plasmodium falciparum*. *J Biol Chem.* 281: 31995–312003.
Tremp A, Dessens J. 2011. Malaria IMC1 membrane skeleton proteins operate autonomously and participate in motility independently of cell shape. *J Biol Chem.* 286:5383–5391.
Tremp A, Khater E, Dessens J. 2008. IMC1b is a putative membrane skeleton protein involved in cell shape, mechanical strength, motility, and infectivity of malaria ookinetes. *J Biol Chem.* 283:27604–27611.
Voss TS, Healer J, Marty AJ, Duffy MF, Thompson JK, Beeson JG, Reeder JC, Crabb BS, Cowman AF. 2006. A var gene promoter controls allelic exclusion of virulence genes in *Plasmodium falciparum* malaria. *Nature* 439:1004–1008.
Wasmuth J, Peregrin-Alvarez J, Finney C, Parkinson J. 2009. The origins of apicomplexan sequence innovation. *Genome Res.* 19:1202–1212.
Xiong X, Song H, On T, Lochovsky L, Provart N, Parkinson J. 2011. PhyloPro: a web-based tool for the generation and visualization of phylogenetic profiles across Eukarya. *Bioinformatics* 27: 877–878.
Yeoman J, Hanssen E, Maier A, Klonis N, Maco B, Baum J, Turnbull L, Whitchurch C, Dixon M, Tilley L. 2011. Tracking Glideosome-associated protein 50 reveals the development and organization of the inner membrane complex of *Plasmodium falciparum*. *Eukaryot Cell.* 10:556–564.